

**ADDRESSING THE RISKS OF TOXIC GAS  
ACCUMULATION IN UNDERGROUND MINES: A  
COMPREHENSIVE APPROACH TO  
VENTILATION, DETECTION, AND WORKER  
SAFETY**

by

MADINA GABDULLIYEVA

THESIS SUPERVISOR

SERGEI SABANOV

Thesis submitted to the School of Mining and Geosciences of  
Nazarbayev University in Partial Fulfillment of the Requirements for the  
Degree of  
**Bachelor of Science in Mining Engineering**

**Nazarbayev University**

**15.04.2025**

## **ORIGINALITY STATEMENT**

I, Madina Gabdulliyeva hereby declare that this submission is my own work and to the best of my knowledge it contains no materials previously published or written by another person, or substantial proportions of material which have been accepted for the award of any other degree or diploma at Nazarbayev University or any other educational institution, except where due acknowledgement is made in the thesis.

Any contribution made to the research by others, with whom I have worked at NU or elsewhere is explicitly acknowledged in the thesis.

I also declare that the intellectual content of this thesis is the product of my own work, except to the extent that assistance from others in the project's design and conception or in style, presentation and linguistic expression is acknowledged.

Signed on 15.04.2025

---

## ABSTRACT

This thesis evaluates the risks associated with the inadequate ventilation of toxic gases in underground mining environments by utilizing a simulation-driven assessment of a real-world, undisclosed room-and-pillar mine layout. The study focuses on four critical airborne contaminants—methane ( $CH_4$ ), carbon monoxide (CO), nitrogen dioxide ( $NO_2$ ), and diesel particulate matter (DPM)—which are routinely generated through geological emissions, methane exposure operations, and diesel equipment activity. These pollutants pose both acute and chronic health hazards, especially when allowed to accumulate in confined mine workings without sufficient dispersion or real-time monitoring.

Traditional gas hazard management strategies, relying on static ventilation designs and threshold-triggered alarm systems, have shown limited adaptability in accounting for dynamic spatial and temporal fluctuations in gas concentrations. To address these limitations, this research adopts a scenario-based simulation approach using Ventsim™ Visual software to model airflow and contaminant behavior under realistic operational conditions. The simulations are conducted within the geometric and infrastructural constraints of a confidential production section from an active room-and-pillar mine, allowing for more accurate representation of field ventilation challenges.

The analysis incorporates secondary data from peer-reviewed studies, regulatory exposure limits, and empirical emission benchmarks to evaluate system performance under three core scenarios: baseline ventilation, post-exposure contaminant release, and localized diesel equipment operation. Results highlight critical ventilation inefficiencies, including persistent stagnation zones and delayed gas clearance times, particularly in regions distal from intake airways. These findings validate the hypothesis that conventional ventilation systems may fall short of regulatory compliance during transient or sustained emission events.

By identifying specific airflow vulnerabilities and pollutant accumulation patterns, the study demonstrates the value of predictive simulation in informing adaptive ventilation strategies. This research contributes to the advancement of intelligent mine safety systems, offering data-informed guidance for improving ventilation efficiency and occupational health protection in underground mining contexts.

## **DEDICATION**

This thesis is dedicated to my family, whose constant support and encouragement have carried me through every step of this journey. To my mother, thank you for believing in me even when I doubted myself, for your patience during long nights and stressful deadlines, and for your unconditional love whenever I needed it.

To my friends and classmates — thank you for keeping me grounded, laughing with me through the chaos, and reminding me that I was not alone in this.

And finally, I dedicate this work to all the miners who work underground every day, often in dangerous conditions. I hope that in some small way, this research can contribute to making their work safer and their lives better.

## **ACKNOWLEDGMENT**

I would like to express my heartfelt gratitude to Nazarbayev University, and especially the School of Mining and Geosciences, for giving me the chance to grow, learn, and challenge myself over the past four years. Being part of this school has been more than just about lectures and labs, it has been a place where I have built lifelong skills, friendships, and memories.

A special thank you goes to all the professors and staff in the School of Mining and Geosciences. Your dedication to teaching, your high standards, and your genuine care for students have shaped the way I think and approach problems. I have learned so much from each of you, not just academically, but also in terms of discipline, integrity, and resilience.

I am especially grateful to my supervisor, Dr. Sergei Sabanov, for his patience, guidance, and honest feedback throughout this project. Thank you for always pointing me in the right direction and for pushing me to think critically, even when the answers weren't easy or obvious.

To my friends and classmates, thank you for being part of this crazy, challenging, and rewarding ride. From study sessions to late-night calls and coffee-fueled deadlines, your support and laughter made the difficult moments bearable and sometimes even fun.

Finally, I want to acknowledge everything that does not show up in the final pages of this thesis, the late nights, the small victories, the frustration, and the persistence it took to keep going. This work is a reflection not just of research, but of growth. I am genuinely thankful to everyone and everything that helped me reach this point.

# TABLE OF CONTENTS

1. INTRODUCTION .....	1
1.1 Background .....	1
1.2 Objectives of the Thesis .....	2
1.2.1 Primary Objective .....	2
1.2.2 Specific Objectives .....	3
1.3 Research Hypotheses .....	3
1.4 Justification of the R&D .....	4
1.5 Scope of Work .....	5
1.6 Practical Importance .....	5
2. LITERATURE REVIEW .....	6
2.1 Toxic Gas Accumulation in Underground Mining Environments .....	7
2.2 Ventilation Strategies and Modeling of Gas Migration .....	8
2.3 Sensor Technologies and Real-Time Gas Monitoring .....	9
2.4 AI and Predictive Modeling in Gas Hazard Detection .....	10
2.5 Safety, Risk Management, and Regulatory Approaches .....	12
2.6 Environmental and Health Perspectives .....	13
2.7 Research Gaps and Technological Limitations .....	14
2.8 Socioeconomic and Operational Dimensions .....	15
2.9 Future Research Directions and Safety System integration .....	16
3. METHODOLOGY .....	18
3.1 Research Design .....	19
3.2 Conceptual Mine Model and Layout .....	20
3.3 Simulation Scenarios and Parameters .....	22
3.3.1 Scenario 1: Baseline Ventilation without Emissions .....	22

3.3.2 Scenario 2: Post-Exposure Contaminant Release .....	22
3.3.3 Scenario 3: Diesel Equipment Operation .....	22
3.3.4 Simulation Parameters and Configuration .....	23
3.3.5 Performance Monitoring and Output Variables .....	24
3.4 Simulation Workflow and Procedure.....	27
3.5 Evaluation Metrics and Output Analysis .....	28
3.6 The use of Ventsim and @Risk Softwares .....	30
4. RESULTS .....	31
4.1 Evaluation Metrics and Output Analysis .....	31
4.2 Post-Exposure Gas Dispersion Results .....	37
4.3 Diesel Equipment Operation.....	45
4.4 Risk Analysis with Volumetric Methane Model .....	48
5. DISCUSSION.....	51
6. CONCLUSIONS .....	53
7. RECOMMENDATIONS.....	54
8. REFERENCES .....	56

## LIST OF FIGURES

Figure 1. The Scheme of the Room & Pillar mining system.....	32
Figure 2. The view on the Topography and the mine layout.....	32
Figure 3. The view on the Topography. ....	33
Figure 4. The view on the Topography from the side / Horizontal View of the Topography.....	33
Figure 5. Oblique topographic rendering highlighting overburden conditions. ....	33
Figure 6. Baseline Ventilation Network System Summary.....	34
Figure 7. Airflow velocity field (Baseline Scenario). ....	35
Figure 8. Static Pressure Distribution in the Mine Ventilation Network (Baseline Scenario).....	36
Figure 9. Initial dynamic simulation without CH <sub>4</sub> .....	36
Figure 10. Dynamic monitor's locations. ....	38
Figure 11. Dynamic Simulation of CH <sub>4</sub> gas at 3 Minutes Post-Exposure at the 1 <sup>st</sup> monitor. ....	39
Figure 12. Dynamic Simulation of CH <sub>4</sub> gas at 10 Minutes Post- Exposure at the 2 <sup>nd</sup> monitor.....	39
Figure 13. Dynamic Simulation of CH <sub>4</sub> gas at 4 Minutes Post- Exposure at the 4 <sup>th</sup> monitor.....	40
Figure 14. Dynamic Simulation of CH <sub>4</sub> gas at 10 Minutes Post- Exposure at the 5 <sup>th</sup> monitor.....	40
Figure 15. Dynamic Simulation of CH <sub>4</sub> gas at 60 Minutes Post- Exposure at the 6 <sup>th</sup> monitor.....	40
Figure 16. Dynamic Simulation of NO <sub>2</sub> gas at 2 Minutes Post- Exposure at the 1 <sup>st</sup> monitor.....	41
Figure 17. Dynamic Simulation of NO <sub>2</sub> gas at 3 Minutes Post- Exposure at the 2 <sup>nd</sup> monitor.....	41

Figure 18. Dynamic Simulation of NO <sub>2</sub> gas at 25 Minutes Post- Exposure at the 3 <sup>rd</sup> monitor.....	42
Figure 19. Dynamic Simulation of NO <sub>2</sub> gas at 23 Minutes Post- Exposure at the 4 <sup>th</sup> monitor.....	42
Figure 20. Dynamic Simulation of NO <sub>2</sub> gas at 45 Minutes Post- Exposure at the 5 <sup>th</sup> monitor.....	42
Figure 21. Dynamic Simulation of NO <sub>2</sub> gas at 65 Minutes Post- Exposure at the 6 <sup>th</sup> monitor.....	43
Figure 22. Dynamic Simulation of CO gas at 2 Minutes Post- Exposure at the 1 <sup>st</sup> monitor. .....	43
Figure 23. Dynamic Simulation of CO gas at 15 Minutes Post- Exposure at the 2 <sup>nd</sup> and 3 <sup>rd</sup> monitors.....	43
Figure 24. Dynamic Simulation of CO gas at 35 Minutes Post- Exposure at the 4 <sup>th</sup> monitor.....	44
Figure 25. Dynamic Simulation of CO gas at 65 Minutes Post- Exposure at the 5 <sup>th</sup> monitor.....	44
Figure 26. Dynamic Simulation of CO gas at 90 Minutes Post- Exposure at the 6 <sup>th</sup> monitor.....	44
Figure 27. Dynamic Simulation of DPM Dispersion at 2 Minutes of Diesel Operation at the 1 <sup>st</sup> monitor.....	46
Figure 28. Dynamic Simulation of DPM Dispersion at 15 Minutes of Diesel Operation at the 2 <sup>nd</sup> and 3 <sup>rd</sup> monitors. ....	47
Figure 29. Dynamic Simulation of DPM Dispersion at 20 Minutes of Diesel Operation at the 4 <sup>th</sup> monitor.....	47
Figure 30. Dynamic Simulation of DPM Dispersion at 30 Minutes of Diesel Operation at the 5 <sup>th</sup> monitor.....	47
Figure 31. Dynamic Simulation of DPM Dispersion at 35 Minutes of Diesel Operation at the 6 <sup>th</sup> monitor.....	48
Figure 33. Exposure of methane as predicted by the Methane Model. ....	49

Figure 34. Fit comparison of methane exposure with Lognormal Distribution Model..	50
Figure 35. Contribution of factors to variance. ....	50
Figure 36. Tornado chart on the inputs.....	51

## LIST OF TABLES

Table 1. Location and functional role of sensor nodes used in the simulation model....	21
Table 2. Key environmental and ventilation parameters used in the simulation.....	23
Table 3. Input variables used in the simulation. ....	25
Table 4. Summary of gas Concentrations Following Methane Gases Exposure Event.	37
Table 5. Summary of DPM Concentrations during Diesel Equipment Operation at LHD Zone. ....	46
Table 6. Values of given inputs to the Methane Model.....	49

# 1. INTRODUCTION

## 1.1 Background

Toxic gas accumulation remains one of the most critical and persistent challenges in underground mining operations. Although mining technologies and safety protocols have evolved significantly over recent decades, the subsurface environment continues to facilitate the release, entrapment, and spatial heterogeneity of hazardous gases. Among the most prominent toxic substances encountered in active underground workings are methane ( $CH_4$ ), carbon monoxide ( $CO$ ), nitrogen dioxide ( $NO_2$ ), and diesel particulate matter (DPM). These gases originate from geological strata, exposure operations, and combustion processes associated with diesel-powered machinery. In the absence of effective dispersion and detection, such contaminants pose acute risks to worker health and operational continuity, and in certain cases, may trigger catastrophic events such as explosions or mass asphyxiation.

Methane is particularly hazardous due to its flammability and explosive potential, with a lower explosive limit (LEL) of approximately 5% by volume in air. Carbon monoxide, a product of incomplete combustion, binds with hemoglobin at rates over 200 times greater than oxygen, leading to hypoxia even at relatively low concentrations. Nitrogen dioxide, often generated during exposure or from diesel exhaust, is a corrosive oxidizer that affects the respiratory system, while DPM is comprising fine aerosols from diesel engines, poses both short and long-term respiratory hazards due to its ultrafine particle size and chemical toxicity. The low visibility, odorless character, and localized behavior of these contaminants further complicate hazard management, especially in areas with limited airflow.

Historically, gas control in underground mining has relied on static ventilation designs and threshold-triggered alarms from fixed-point gas detectors. While adequate for baseline conditions, these systems often fail to adapt to real-time fluctuations in gas release, equipment movement, or localized stagnation zones. Manual inspections and delay-prone alarm systems may detect hazards only after critical thresholds have been breached, offering insufficient protection in rapidly evolving scenarios such as exposure or diesel-intensive operations.

In response, the industry has seen increasing interest in dynamic ventilation strategies supported by wireless sensor networks and simulation-based planning tools, such as Ventsim™. Ventsim™ is a widely adopted software platform, offers capabilities for modeling airflow behavior, thermal interactions, and gas transport under both steady-state and transient conditions. However, its potential remains underutilized in analyzing multi-gas dispersion under practical, scenario-based constraints—particularly those involving simultaneous sources, delayed clearance zones, and geometrically complex ventilation pathways.

To address this gap, the present study simulates gas dispersion and airflow dynamics within a confidential, real-world room-and-pillar mine layout using Ventsim's advanced modeling capabilities. The selected geometry provides a field-calibrated spatial framework for evaluating risks associated with incomplete ventilation of  $CH_4$ ,  $CO$ ,  $NO_2$  and DPM. The approach employs dynamic, scenario-specific simulations that reflect realistic post-exposure conditions and diesel equipment operation cycles. The resulting airflow, gas concentration, and thermal interaction patterns are analyzed to identify ventilation inefficiencies and to inform more adaptive and targeted air quality management practices.

## **1.2 Objectives of the Thesis**

### **1.2.1 Primary Objective**

This research aims to evaluate the performance and limitations of underground ventilation systems in managing toxic gas dispersion under realistic, dynamically evolving operational conditions. A confidentially sourced, real-world room-and-pillar mine layout is used as the simulation domain, providing a practical and spatially constrained context for modeling ventilation behavior and gas migration. Through the application of Ventsim™ software, the study assesses how well existing ventilation configurations respond to high-risk scenarios involving post-exposure gas surges and continuous diesel machinery emissions. The overarching goal is to develop a scenario-driven simulation framework that supports adaptive ventilation planning and risk-informed decision-making.

### 1.2.2 Specific Objectives

This study investigates the feasibility of integrating advanced simulation tools, scenario-specific emission modeling, and spatial hazard analysis to mitigate the accumulation of airborne contaminants in underground mining environments. Drawing upon current regulatory guidelines, peer-reviewed literature, and industry-standard operational parameters, the research focuses on the behavior of four critical pollutants—methane ( $CH_4$ ), carbon monoxide ( $CO$ ), nitrogen dioxide ( $NO_2$ ), and diesel particulate matter (DPM)—under variable airflow conditions. Specifically, the objectives are:

- 1) To simulate baseline steady-state airflow and pressure distributions within an undisclosed room-and-pillar mine layout using Ventsim™, establishing a reference for ventilation adequacy in the absence of emissions.
- 2) To model the dynamic dispersion of  $CH_4$ ,  $CO$ ,  $NO_2$  following a controlled gas exposure event, capturing short-term fluctuations in concentration and evaluating clearance times relative to occupational exposure limits.
- 3) To simulate DPM and associated gas emissions from diesel equipment operating at multiple drift locations, examining how geometry, emission location, and ventilation influence the persistence and spread of contaminants.
- 4) To simulate Methane Model using Risk Analysis with Volumetric Reserves 3 with the varying inputs taken to reproduce real-life scenarios and make correlation with the Ventsim™ simulation.

### 1.3 Research Hypotheses

1) Scenario-Induced Accumulation: Transient high-emission events, such as gas exposure or localized diesel equipment use, will generate elevated concentrations of  $CH_4$ ,  $CO$ ,  $NO_2$  and DPM that exceed regulatory thresholds in areas with limited ventilation coverage or suboptimal airflow dynamics.

2) Limitations of Baseline Modeling: While steady-state ventilation simulations may demonstrate compliance with design airflow and pressure specifications, they will

fail to reveal the spatially localized or temporally evolving zones of toxic gas accumulation that arise during operational disturbances.

3) Predictive Utility of Dynamic Simulation: Ventsim™-based dynamic modeling provides a reliable platform for simulating gas behavior and identifying ventilation inefficiencies, enabling scenario-specific modifications to airflow patterns that improve contaminant clearance and reduce occupational exposure risks.

## **1.4 Justification of the R&D**

This research responds to an urgent operational need for scenario-driven ventilation analysis frameworks capable of capturing the transient dynamics of airborne contaminants within complex underground mining environments. While many underground mines meet regulatory airflow and pressure requirements under steady-state conditions, such static designs frequently underperform during short-term high-emission events, including post-exposure gas releases and diesel equipment operations. Utilizing an undisclosed but operationally representative room-and-pillar mine layout, this study applies Ventsim™ to simulate the dispersion and clearance of four critical toxic agents—methane ( $CH_4$ ), carbon monoxide ( $CO$ ), nitrogen dioxide ( $NO_2$ ), and diesel particulate matter (DPM)—across various emission-driven scenarios.

By modeling pollutant behavior under time-sensitive operating conditions, the research offers a granular assessment of ventilation responsiveness, contaminant accumulation zones, and clearance efficiency. The results reveal key limitations of conventional fixed ventilation networks, particularly in their inability to accommodate spatiotemporal variations in gas concentrations. In contrast, the simulation-driven methodology employed here demonstrates the potential of predictive modeling to inform targeted airflow optimization, thereby supporting proactive, risk-aware ventilation planning.

Moreover, this approach aligns with broader industry goals related to sustainability and energy efficiency by enabling airflow calibration that minimizes redundancy while maintaining compliance with occupational exposure standards. Beyond its technical contributions, the study advances the strategic integration of digital ventilation systems into next-generation intelligent mining frameworks, offering a

replicable model for enhancing underground air quality management through simulation-based design and scenario validation.

## 1.5 Scope of Work

This study is limited to a simulation-based evaluation and does not incorporate empirical field measurements or in-situ sensor deployment. All analyses are conducted within a digitally reconstructed section of an undisclosed room-and-pillar underground mine, developed using geometry and airflow parameters informed by regulatory guidelines and peer-reviewed literature. The simulation environment is designed to reflect realistic mining conditions while ensuring computational control and reproducibility. The investigation focuses on three operational scenarios that typify ventilation challenges in modern underground mining:

1. A baseline scenario, representing steady-state airflow distribution under normal, non-emission conditions;
2. A post-exposure scenario, simulating the rapid release and spatial dispersion of  $CH_4$ ,  $CO$  and  $NO_2$  following a detonation event;
3. A diesel equipment operation scenario, reflecting sustained emissions of  $CH_4$ ,  $CO$ ,  $NO_2$  and DPM during localized LHD activity.

Each scenario includes elevated input concentrations of methane, carbon monoxide, nitrogen dioxide, and diesel particulate matter (DPM), consistent with worst-case but literature-supported exposure events. Using Ventsim™, the study models transient airflow behavior, pressure differentials, and contaminant dispersion over a time-stepped simulation window. Comparative analysis across scenarios enables a critical assessment of how traditional ventilation configurations perform under dynamic stress conditions, providing insights into system vulnerabilities and opportunities for improvement through predictive simulation.

## 1.6 Practical Importance

The practical significance of this research is anchored in its contribution to enhancing occupational health and ventilation performance within underground mining environments. In spatially constrained and airflow-sensitive domains such as room-and-pillar mines, even incremental improvements in gas dispersion modeling, hazard

forecasting, and airflow control can meaningfully reduce the incidence of acute toxic exposures and long-term respiratory health risks. By simulating the behavior of methane ( $CH_4$ ), carbon monoxide ( $CO$ ), nitrogen dioxide ( $NO_2$ ), and diesel particulate matter (DPM) under dynamic operational conditions, this study provides actionable insights into the ventilation responses required during high-risk events—including post-exposure contamination and prolonged diesel machinery deployment.

For mine operators and ventilation engineers, the use of Ventsim™ as a scenario-testing tool offers a replicable and non-invasive means of diagnosing airflow inefficiencies, forecasting hazard zones, and pre-emptively adapting ventilation strategies to mitigate exposure. This capability enhances operational resilience by reducing the frequency of unplanned ventilation interventions and production downtime, while also lowering the risk of non-compliance with occupational exposure regulations. The use of a simulated section of an undisclosed room-and-pillar mine supports generalizability of findings while preserving operational confidentiality.

On a regulatory level, the findings have potential utility in shaping updated guidelines for gas threshold monitoring, emission response protocols, and ventilation system design under variable loading conditions. Furthermore, the integrated simulation framework contributes to the ongoing development of intelligent mining systems—by demonstrating the practical application of predictive modeling, digital airflow analytics, and operational scenario integration in the context of ventilation planning. These contributions align with industry-wide objectives for enhanced automation, energy efficiency, and proactive occupational safety management in next-generation mining operations.

## **2. LITERATURE REVIEW**

This literature review is organized into nine thematic sections that collectively examine the multifaceted nature of toxic gas hazards in underground mining. Section 2.1 discusses the geomechanical and chemical processes underlying gas accumulation in subsurface environments. Section 2.2 evaluates the role of ventilation strategies and gas migration modeling, while Section 2.3 explores the development and application of real-time gas detection technologies. Section 2.4 focuses on artificial intelligence and predictive analytics in hazard forecasting. Section 2.5 addresses the regulatory

frameworks and risk management approaches relevant to mine safety. Section 2.6 expands the scope to include environmental and health perspectives. Section 2.7 identifies current research limitations and technological challenges. Section 2.8 considers the socioeconomic and operational implications of gas hazard mitigation, and finally, Section 2.9 outlines emerging trends and future research directions related to integrated safety systems.

## **2.1 Toxic Gas Accumulation in Underground Mining Environments**

The accumulation of toxic gases in underground mines represents a longstanding and multifaceted challenge in the mining industry. These gases—principally methane ( $CH_4$ ), carbon monoxide ( $CO$ ), hydrogen sulfide ( $H_2S$ ), and nitrogen oxides—emerge from geomechanical strata, combustion processes, or diesel engine exhaust. The closed and often poorly ventilated geometry of underground excavations exacerbates danger, allowing for the stratification and stagnation of harmful gases in specific zones. While conventional studies have identified the sources and hazards associated with toxic gas accumulation, emerging literature points toward more nuanced spatial and temporal factors.

Menéndez et al. (2022) analyzed gas distribution patterns under different ventilation configurations, emphasizing that local variations in airflow contribute significantly to gas propagation. Their findings revealed that even within active ventilation networks, pockets of methane and carbon monoxide can concentrate due to directional changes, pressure drops, or geometric constraints. These results are consistent with observations by Wang et al. (2022), who investigated gas distribution in goafs and identified that gas migration patterns are governed by residual voids and the dynamic evolution of surrounding rock structures.

Zheng et al. (2019) provided a comprehensive review of coalbed methane emissions and drainage practices, highlighting that geotechnical variability plays a pivotal role in emission rates and control effectiveness. Although numerous drainage techniques have been proposed, the applicability and efficiency of each depend on context. Their study further examined emission source behavior across different coal seams, linking gas liberation potential to structural and thermal gradients within the strata.

Post-incident gas behavior is another critical dimension, especially in mines susceptible to spontaneous combustion or explosive gas release. Ge et al. (2024) introduced a mobile fire-extinguishing method utilizing liquid carbon dioxide and demonstrated its capacity to displace and suppress gas-rich environments following combustion events. Complementing this, Huang et al. (2025) investigated the dynamics of harmful gas groups post-explosion, uncovering that residual gas migration poses prolonged risks even after the primary event has subsided. Their research offers detailed insights into delayed gas redistribution and ventilation design adaptations.

The role of external factors such as seasonal variability, barometric pressure, and deep mine thermal gradients further complicates the risk landscape. Ziętek et al. (2020) developed a portable environmental monitoring system, revealing that temperature and ventilation interplay significantly affect gas dispersion rates. Similar insights were offered by Yang et al. (2020), who assessed hazard dispersion in salt-rock storage caverns, a geologic analog to deep mine voids. Their findings reinforced the importance of accounting for gas density differentials in both risk prediction and sensor placement.

## **2.2 Ventilation Strategies and Modeling of Gas Migration**

Ventilation design in underground mines serves as the principal control mechanism for diluting and expelling hazardous gases. The dynamic conditions within mine environments necessitate adaptive and robust ventilation frameworks capable of addressing spatial variability and real-time operational demands. Traditional design methodologies based on steady-state assumptions are increasingly complemented by simulation tools and sensor-integrated systems that enable real-time response and optimization.

Rahimi et al. (2022) applied computational fluid dynamics (CFD) modeling to assess the effects of gas content variability on methane distribution in mine roadways. Their work highlighted how changes in input gas concentrations influence the spatial extent and intensity of methane accumulation. Through simulated airflow patterns, they identified areas of potential gas entrapment, providing quantitative insights into airflow pathway optimization.

Semin and Kormshchikov (2024) reviewed recent advancements in artificial intelligence integration with mine ventilation systems. Their findings point to the growing

relevance of machine learning techniques for predicting airflow behavior and automating ventilation adjustments. These intelligent systems are particularly beneficial in deep or complex mine geometries where conventional designs are insufficient.

Chang et al. (2024) proposed a multi-sensor forecasting model tailored to longwall face conditions. Their model demonstrated how real-time data could be harnessed to develop predictive safety warning strategies that dynamically alter ventilation patterns. By fusing sensor data with control algorithms, their study represents a shift from reactive to anticipatory safety management.

Jo et al. (2018) introduced a fiber Bragg grating-based condition monitoring system capable of detecting structural and atmospheric changes in coal mines. Integrated into ventilation infrastructures, such systems enhance the responsiveness of gas control mechanisms by triggering ventilation recalibrations in response to evolving subsurface conditions.

Krause and Krzemień (2014) developed a risk assessment approach based on expert panel surveys to evaluate ventilation system effectiveness against methane hazards. Their structured framework provided a basis for semi-quantitative evaluation of airflow performance across various mining scenarios. The study emphasized the utility of expert-driven evaluation in scenarios lacking comprehensive sensor networks.

Anas et al. (2017) explored wireless technologies for ventilation monitoring, demonstrating their feasibility for remote airflow diagnostics and automated feedback control. Their results showcased the scalability and operational flexibility of wireless systems in real-time hazard mitigation.

## **2.3 Sensor Technologies and Real-Time Gas Monitoring**

The advancement of sensor-based technologies has transformed underground mine safety by enabling real-time detection and continuous monitoring of hazardous gases. This transition from manual sampling to autonomous sensor networks has been facilitated by innovations in optoelectronics, wireless data transmission, and integrated system design. Sensor technologies are now integral components of comprehensive hazard mitigation systems, facilitating rapid detection, quantification, and communication of gas concentration data within complex subsurface environments.

Chen et al. (2022) proposed an optically powered gas monitoring system utilizing single-mode fibre, tailored for underground coal mines. The system's design offered high sensitivity and immunity to electromagnetic interference, which is particularly valuable in environments with heavy machinery and metallic infrastructure. This approach enabled continuous monitoring without the limitations of conventional battery-powered sensors.

Gong et al. (2022) conducted a systematic evaluation of laser gas sensors used in intelligent coal mining operations. Their study outlined the operating principles of tunable diode laser absorption spectroscopy (TDLAS) and quartz-enhanced photoacoustic spectroscopy (QEPAS), both of which enable precise, fast-response measurements of methane and carbon monoxide in complex gas mixtures. These technologies support early detection and allow for proactive intervention in gas-prone sections of the mine.

Osunmakinde (2013) developed a wireless sensor network (WSN) architecture for toxic gas monitoring, focusing on low-power operation and spatial coverage. The system employed adaptive routing protocols to maintain data integrity in interference-prone environments, making it suitable for extended deployments in deep mining sections. The application demonstrated the viability of scalable, decentralized gas monitoring systems that operate autonomously in real time.

Sadeghi et al. (2022) presented a systematic review of wireless sensor network applications in occupational safety, with specific attention to underground mining environments. Their analysis included energy efficiency, network lifetime, and fault tolerance as critical parameters in sensor deployment. They also emphasized the role of sensor redundancy and spatial distribution in minimizing blind spots in gas concentration mapping.

Keshamoni et al. (2024) developed an IoT-enabled gas detection platform incorporating automatic regulator control. The proposed system was capable of detecting multiple gases simultaneously and adjusting ventilation or alarm systems accordingly. This integration of sensing and actuation mechanisms illustrates the evolution toward fully autonomous hazard mitigation infrastructure in underground mining.

## **2.4 AI and Predictive Modeling in Gas Hazard Detection**

The application of artificial intelligence (AI) and machine learning (ML) in gas hazard detection has become a focal point in the modernization of underground mine

safety systems. These technologies facilitate predictive modeling by identifying spatiotemporal patterns in gas concentration data, enabling early warnings and adaptive responses. The integration of AI with sensor networks and multivariate data sources forms the foundation of next-generation safety infrastructures.

Tutak et al. (2024) developed a multi-layer perception (MLP) neural network to predict methane concentrations in underground coal mines using historical gas monitoring data. Their model demonstrated high accuracy and real-time adaptability, allowing for proactive intervention in hazardous conditions. The neural network was trained on large-scale datasets obtained from operational monitoring systems, showcasing the practicality of supervised learning algorithms in underground applications.

Wu et al. (2024) performed a comparative analysis of ten machine learning algorithms for short-term gas concentration forecasting. Their study evaluated model performance based on prediction accuracy, computation time, and robustness to sensor noise. Ensemble learning techniques, particularly random forest and gradient boosting, outperformed other models under variable mining conditions, highlighting the relevance of hybrid AI architectures.

Ma et al. (2020) introduced an edge computing framework for distributed gas concentration prediction. Their system combined real-time sensing with localized data processing, reducing latency and ensuring uninterrupted operation in deep or communication-constrained mine sections. The edge AI approach enabled rapid anomaly detection without reliance on centralized computing infrastructure.

Sharma and Maity (2024) reviewed ML-based gas hazard identification techniques in coal mines, covering classification, regression, and clustering methods. They emphasized the increasing role of unsupervised learning for anomaly detection in sparse or incomplete datasets, a common issue in underground sensor networks. Their analysis also pointed to the importance of algorithm interpretability for operator trust and regulatory compliance.

Narkhede et al. (2021) explored sensor fusion using multimodal AI to enhance gas detection accuracy. By combining data from temperature, humidity, and gas-specific sensors, the system minimized false positives and improved decision-making precision. Their results validated the effectiveness of multimodal learning strategies in environments with overlapping hazard signals.

Liang et al. (2024) extended the application of multimodal data fusion to geohazard prediction, integrating gas concentration data with structural and geomechanical indicators. Their model utilized deep learning to correlate multiple hazard parameters and generate risk forecasts. The incorporation of heterogeneous data sources offered a more holistic understanding of underground safety dynamics.

All the previously done researches lack something in their ML and AI-based gas detection techniques. Some of them are constrained by incomplete datasets, which exclude critical environmental or geomechanical variables (Sharma & Maity, 2024). Also, even though these techniques cover the theoretical data from old sources, many computational models have not been validated under real mining conditions, leading to discrepancies between predicted and observed gas behaviors (Wu et al., 2022).

## **2.5 Safety, Risk Management, and Regulatory Approaches**

The regulatory and managerial dimensions of gas hazard mitigation in underground mining are central to ensuring worker safety and operational continuity. Safety standards and risk assessment methodologies have evolved in response to technological advancements, shifting from reactive frameworks to systems-based preventive strategies. In parallel, the role of policy and governance in enforcing compliance with ventilation, monitoring, and evacuation procedures has grown increasingly prominent.

Asfaw et al. (2013) analyzed the relationship between occupational injuries and profitability in U.S. underground coal mines, revealing that firms with stronger safety performance tend to be more economically viable. Their empirical investigation established that investment in safety infrastructure, including gas monitoring and ventilation systems, correlates with both human and financial outcomes, reinforcing the need for integrated safety-economic policies.

Jia and Nie (2017) examined the effects of decentralization and collusion on coal mine fatalities, demonstrating how weak governance structures contribute to regulatory evasion and safety violations. Their findings highlighted that political fragmentation and lack of enforcement capacity can undermine the effectiveness of technical interventions, emphasizing the role of institutional integrity in hazard control.

Olczak et al. (2023) conducted a global review of methane policies, identifying that only a small proportion of emissions are regulated through comprehensive frameworks. They noted significant variation in regulatory coverage, stringency, and transparency across jurisdictions. The study underscored the need for harmonized international standards and the integration of methane control into environmental and occupational health policy agendas.

Karacan et al. (2011) provided a detailed review of coal mine methane capture and utilization strategies. They classified drainage and ventilation practices based on their safety and environmental benefits, illustrating how methane management can serve dual purposes in risk reduction and climate mitigation. Their review also documented the historical development of gas control protocols, offering context for current best practices.

## **2.6 Environmental and Health Perspectives**

Toxic gas hazards in underground mining have far-reaching implications not only for operational safety but also for environmental sustainability and occupational health. The dual burden of acute exposure to harmful gases and chronic environmental degradation necessitates a broader evaluative framework that encompasses physiological risk, ecological impacts, and mitigation strategies aligned with sustainability objectives.

Fan and Xu (2021) assessed occupational health risks associated with chemical exposure in coal mines by employing a deep learning-based risk evaluation model. Their work underscored the complexity of exposure scenarios and highlighted the need for individualized risk assessments based on temporal exposure profiles. Their methodology integrated real-time monitoring data with predictive analytics to inform worker safety protocols.

Anas et al. (2017) examined gas testing and monitoring methods using wireless technologies, with a focus on real-time diagnostics. Their study demonstrated the importance of dynamic hazard identification for protecting worker health in high-risk zones, particularly during excavation and  $CH_4$  gas exposure phases. The integration of wireless communication tools enabled responsive safety interventions without delay.

Kumar et al. (2013) provided a detailed overview of gas monitoring sensor applications in hazardous areas, identifying their role in reducing exposure to harmful gases such as methane and carbon monoxide. Their findings emphasized that continuous sensor-based surveillance significantly lowers the probability of long-term exposure effects, contributing to the reduction of chronic respiratory conditions among underground workers.

These contributions illustrate the convergence of health science, engineering, and environmental policy in addressing gas-related risks. As mining operations become increasingly automated and sensor-dependent, understanding the physiological and ecological consequences of gas exposure remains a critical area of research and operational focus.

## **2.7 Research Gaps and Technological Limitations**

Despite considerable progress in gas detection, ventilation design, and predictive analytics, a number of persistent research gaps and technological limitations continue to constrain the effectiveness of gas hazard mitigation in underground mining. These limitations span from incomplete modeling assumptions to practical deployment challenges in dynamic subsurface environments.

Raheem (2011) highlighted the absence of robust real-time monitoring systems in remote or high-risk zones, noting that coverage gaps often emerge due to sensor placement limitations and communication signal degradation. Inconsistent monitoring not only affects response times but also leads to underestimation of toxic gas concentrations in localized hotspots.

Wu et al. (2022) conducted a study on gas explosion product migration in complex mine air networks and reported significant difficulties in simulating the precise flow of combustion products. Their findings indicated that current CFD models struggle to account for turbulent and multi-phase flow dynamics, particularly during post-explosion scenarios, which limit the accuracy of predictive safety systems.

Limitations in data integration are also evident. While AI and machine learning models have demonstrated predictive capabilities, many still rely on narrowly defined datasets that exclude critical environmental or geomechanical variables. Furthermore,

model interpretability remains an issue, making it difficult for mine operators to validate AI-driven decisions within regulatory frameworks.

Energy constraints and hardware robustness continue to affect the long-term deployment of wireless sensor networks in harsh underground conditions. Issues such as battery degradation, electromagnetic interference, and mechanical wear reduce sensor lifespan and data reliability, particularly in deeper mines where maintenance access is limited.

In addition, many studies prioritize methane and carbon monoxide, often neglecting gases such as hydrogen sulfide and nitrogen dioxide, which pose significant health risks even at low concentrations. This selective focus results in a fragmented understanding of total gas exposure and leaves certain hazard scenarios underexplored.

There is also a notable lack of field validation for many computational models. Laboratory-scale simulations are often not tested under real mining conditions, leading to discrepancies between predicted and observed gas behaviors. This gap hinders the development of universally applicable ventilation and detection protocols.

## **2.8 Socioeconomic and Operational Dimensions**

Gas hazard management in underground mining intersects with broader socioeconomic and operational considerations, including workforce safety, productivity, capital investment, and the public perception of mining activities. These dimensions shape the implementation, acceptance, and long-term sustainability of gas mitigation technologies across diverse mining contexts.

Chečko et al. (2021) examined gas migration risks in mines undergoing closure and emphasized the socioeconomic implications of residual gas accumulation in decommissioned workings. Their findings highlighted the necessity for post-closure gas monitoring policies, particularly in densely populated regions where abandoned mines may continue to pose latent hazards. This perspective underscores the long-term societal responsibility associated with mine safety management.

Vallejo-Molina et al. (2024) developed an AI-based alert system for explosion prediction in Colombian underground mines, incorporating stakeholder feedback in system design. Their approach reflected an operational shift toward participatory

technology development, where miners, engineers, and policymakers collaboratively influence system functionality. Such integration of local knowledge enhances system usability and fosters a culture of safety.

From an economic standpoint, gas hazard mitigation involves substantial investment in infrastructure, including sensors, ventilation systems, and computational platforms. The alignment of these expenditures with regulatory compliance and insurance incentives can influence company behavior, especially in jurisdictions with stringent safety mandates. The integration of safety systems with productivity monitoring further supports business cases for technology adoption.

Operationally, the deployment of advanced technologies demands workforce training and interdisciplinary collaboration. The use of machine learning algorithms, edge computing devices, and wireless sensor networks requires not only technical expertise but also procedural adaptation on the part of mine personnel. These transitions may be constrained by institutional inertia or limited resource availability in small- and medium-scale operations.

## **2.9 Future Research Directions and Safety System integration**

Gas hazard mitigation in underground mining is likely to evolve through the convergence of digital technologies, systems integration, and interdisciplinary research. As mining operations become increasingly data-rich and operationally complex, there is a discernible shift from discrete technological applications to more unified safety architectures. These frameworks incorporate sensing, prediction, ventilation control, and human decision-making into coordinated systems.

As discussed in Section 2.4, Lin et al. (2020) introduced an AI-based real-time methane prediction system for longwall coal mines, demonstrating the technical feasibility of forecasting gas concentrations using deep learning algorithms. The use of continuous sensor inputs provided a foundation for automated response systems. However, the integration of such systems with existing ventilation infrastructures, as explored in Section 2.2, remains an area requiring further empirical validation and standardization.

Zhang et al. (2020) developed a distributed edge-computing model for gas forecasting, combining localized processing with centralized oversight. This architecture

was found to be robust under limited connectivity conditions, suggesting its applicability in remote or infrastructure-constrained mining operations. While these systems offer potential scalability, their performance under heterogeneous environmental conditions warrants further examination.

Jo et al. (2018), referenced in Section 2.2, presented a fiber Bragg grating-based monitoring system for structural and atmospheric assessment. This approach highlights the movement toward integrated cyber-physical systems capable of continuous environmental sensing and control. Their findings underscore the potential for such systems to augment ventilation safety strategies, though long-term durability and interoperability remain subjects of ongoing research.

Digital twin technologies are increasingly considered in planning frameworks, allowing for the simulation of gas behavior across a range of operational scenarios. As noted in Section 2.6, such tools may facilitate risk assessment and emergency planning. However, challenges related to model calibration, data fidelity, and computational demand persist.

Future studies may benefit from cross-disciplinary efforts involving engineers, data scientists, and occupational health specialists. Priority areas include the development of interpretable AI models for safety-critical decisions, standardization of cross-platform communication protocols, and expanded monitoring of less frequently addressed gases, such as nitrogen dioxide and hydrogen sulfide (see Section 2.7).

Another trajectory involves addressing the environmental footprint of safety systems. Areas of inquiry include low-energy sensor platforms, recyclable materials, and the alignment of gas hazard mitigation with broader ESG (Environmental, Social, and Governance) metrics. While promising in principle, the practical trade-offs between sustainability and operational reliability require further evaluation.

The progression of gas hazard management will depend not solely on technological innovation, but on the integration of regulatory, organizational, and technical frameworks. Insights across Sections 2.3 through 2.8 suggest that future systems will need to balance precision, adaptability, and practicality under the constraints of diverse mining environments.

### 3. METHODOLOGY

The methodological framework of this research is structured around a simulation-based assessment of toxic gas accumulation and ventilation dynamics within a representative room-and-pillar underground mining environment. Building on the critical insights established in the literature review, this chapter presents a detailed and systematic approach for evaluating airflow performance and contaminant behavior using Ventsim™ Visual, a widely recognized software platform for mine ventilation modeling. Given the absence of field measurements or real-time sensor deployment, the study adopts a hypothetical scenario-based design, grounded in peer-reviewed literature and industry-validated ventilation parameters, to ensure both experimental control and contextual relevance to actual mining operations.

The chapter is organized into a sequence of logically connected sections. It begins by outlining the simulation rationale and justifies the use of digital modeling as an effective proxy for dynamic mine ventilation experimentation. A comprehensive conceptualization of the mine model follows, including the geometrical dimensions, airway layout, and ventilation infrastructure underpinning all simulated scenarios. Subsequently, the key operational cases are introduced, focusing on time-sensitive gas dispersion events—namely, post-exposure contaminant release and localized diesel equipment emissions—that represent realistic occupational risk conditions.

The simulation setup section details the configuration and input parameters employed in Ventsim™, including airflow velocity inputs, contaminant injection rates, gas-specific concentration thresholds ( $CH_4$ ,  $CO$ ,  $NO_2$  and DPM), and relevant boundary conditions. A stepwise procedural workflow is presented to promote methodological transparency and facilitate reproducibility. Evaluation metrics such as pressure differentials, airflow vector stability, and contaminant concentration gradients are then defined for comparative analysis across scenarios.

Through this structured simulation approach, the study aims to critically assess the adaptability of conventional ventilation designs and explore opportunities for enhancing gas hazard mitigation through evidence-based digital modeling. The outputs are intended to inform future development of intelligent ventilation strategies capable of supporting both safety and sustainability in underground mining operations.

### 3.1 Research Design

This study employs a simulation-based engineering methodology to analyze toxic gas dispersion, thermal interactions, and ventilation performance within a geometrically defined production section of an undisclosed room-and-pillar underground mine. Rather than representing a complete mine system, the simulation focuses on a single production block that reflects a realistic operational scale, enabling detailed scenario evaluation while preserving computational efficiency. This localized modeling approach allows for the capture of complex ventilation behaviors and contaminant transport mechanisms under dynamic operating conditions, including transient post-exposure gas surges and sustained emissions from diesel load-haul-dump (LHD) equipment.

The simulated mine section measures approximately 4644 meters in length and 1140 meters in width, configured with uniformly spaced drifts and crosscuts. Each tunnel maintains a constant width of 6.9 meters and an average height of 2.7 meters, forming a ventilation volume consistent with mid-scale mechanized hard rock mining operations. The simulated depth is fixed at 263 meters, yielding an ambient atmospheric pressure of approximately 98.4 kPa based on standard barometric lapse rates (Menéndez et al., 2022). A single intake airway is positioned on the western boundary, while the return airway is located on the eastern edge, establishing a longitudinal airflow pathway aligned with real-world ventilation conventions. To monitor spatiotemporal variations in airflow and contaminant concentrations, five sensor nodes are distributed evenly along one central entry, allowing for structured evaluation of pollutant migration, clearance times, and ventilation effectiveness under varying emission scenarios.

Three distinct operational cases are examined:

- 1) A baseline steady-state ventilation model, representing normal airflow without contaminant sources;
- 2) A diesel operation scenario, simulating emissions from an operating LHD unit that generates  $350 \mu\text{g}/\text{m}^3$  of diesel particulate matter, 30 ppm CO, and heat dissipation of approximately 7.5 kW, introduced at two different working zones in the layout (Tutak et al., 2024; Kumar et al., 2013).

Contaminant behavior is simulated dynamically using Ventsim Visual™ with its contaminant and thermal dispersion modules. Gas transport is modeled as passive

dispersion, with no reactive chemistry, and air resistance is calculated using Atkinson's equation. Environmental conditions are set at 22°C air temperature, 65% relative humidity, and rock thermal conductivity of 2.5 W/m·K. Fan curves and boundary pressures are defined based on typical equipment parameters to achieve target airflow velocities within main and auxiliary drifts.

The input parameters for each toxic substance— $CH_4$ ,  $CO$ ,  $NO_2$  and DPM—are summarized in Table 4, with concentration values selected based on recent occupational exposure literature and regulatory benchmarks. Model outputs are analyzed against safety thresholds recommended by the Occupational Safety and Health Administration (OSHA) and the Mine Safety and Health Administration (MSHA), including  $CO$  TWA limits of 50 ppm,  $NO_2$  ceiling values of 5 ppm, and DPM reference levels of 160  $\mu\text{g}/\text{m}^3$ . Key simulation metrics include peak contaminant concentrations at sensor locations, gas clearance times, airflow velocity profiles, and the identification of ventilation dead zones where contaminants may persist.

### **3.2 Conceptual Mine Model and Layout**

The conceptual layout used in this study represents a geometrically simplified yet functionally representative production segment of an undisclosed room-and-pillar underground mine. While not replicating a specific mine site, the model is designed to preserve critical spatial characteristics that influence airflow distribution, contaminant transport, and thermal interactions. This abstraction allows for computational efficiency while maintaining the geometric fidelity necessary to investigate localized gas accumulation, airflow stagnation, and pollutant clearance across interconnected mine headings.

The detonation site is located in the northeastern zone of the layout and is modeled as the primary source of post-exposure emissions, where carbon monoxide ( $CO$ ), nitrogen dioxide ( $NO_2$ ) and methane ( $CH_4$ ) are introduced simultaneously to simulate transient accumulation and subsequent dilution. Central entries are designated as diesel activity zones, where load-haul-dump (LHD) units operate sequentially, and generating continuous emissions of  $CO$  and diesel particulate matter (DPM). By distributing the sources across spatially distinct headings, the model facilitates evaluation of dispersion

dynamics under both sudden ( $CH_4$  exposure) and sustained (diesel operation) emission scenarios, reflecting operational conditions observed in active underground mines.

To support performance monitoring and hazard assessment, five fixed virtual gas sensors are embedded along the central entry, spaced at regular intervals from the intake to the return side of the model. These sensors are configured to capture airflow velocities, temperature changes, and real-time concentrations of  $CH_4$ ,  $CO$ ,  $NO_2$  and DPM under various simulation stages. This spatial sensor configuration enables the evaluation of temporal trends, exposure duration, and pollutant clearance efficiency relative to regulatory thresholds. Sensor placement and operational roles are detailed in Table 1.

**Table 1. Location and functional role of sensor nodes used in the simulation model.**

Sensor Node	Location	Primary Monitoring function
Intake Airway Node	Monitor #1	Records baseline airflow velocity and contaminant-free intake conditions
Early Operation Zone Node	Monitor #3	Monitors initial gas accumulation and airflow behavior under early-phase emission conditions
Midpoint Junction Node	Monitor #4	Detects potential stagnation zones and intermediate gas concentrations
LHD Operation Node	Monitors #2 and #5	Captures CO and DPM levels generated by diesel machinery activity
Return Airway Node	Monitor #6	Assesses overall ventilation performance and contaminant removal efficiency at the exit point

### **3.3 Simulation Scenarios and Parameters**

The simulation phase of this research comprises three operational scenarios, each representing a common source of toxic gas release and thermal load generation in underground mining. These scenarios are modeled within a room and pillar layout using Ventsim Visual™, with all geometric, thermodynamic, and contaminant input values derived from peer-reviewed literature. The selected cases were designed to assess ventilation behavior under steady-state and dynamic conditions while evaluating compliance with regulatory exposure limits.

#### ***3.3.1 Scenario 1: Baseline Ventilation without Emissions***

This initial scenario establishes steady-state airflow conditions across the mine layout without introducing any heat or contaminant sources. It serves as a baseline model to validate ventilation efficiency under nominal operating conditions, define airflow velocity vectors, and identify zones of stagnant or low-velocity flow. The fan configuration, airway resistances, and ventilation boundary conditions remain consistent across all three scenarios to enable controlled cross-scenario comparisons.

#### ***3.3.2 Scenario 2: Post-Exposure Contaminant Release***

The second scenario simulates gas explosion happened near Monitor #1 which is shown also in the following figures. Literature-supported values of  $CH_4$ ,  $CO$ ,  $NO_2$  and DPM will be integrated (Ge et al., 2024; Huang et al., 2025). The release is treated as an instantaneous emission within 120 minutes decay window. This scenario evaluates the system's ability to evacuate hazardous combustion products from the methane exposure site and adjacent drifts, with gas concentrations monitored across six sensor nodes.

#### ***3.3.3 Scenario 3: Diesel Equipment Operation***

The third scenario introduces emissions and heat loads from a diesel-powered load-haul-dump (LHD) unit operating in the midsection of Entry 1. The emissions include 50 ppm carbon monoxide ( $CO$ ), 200 mg/m<sup>3</sup> diesel particulate matter (DPM), and a thermal load of approximately 7.5 kW per LHD unit during peak operation (Fan & Xu, 2021; Kumar et al., 2013). These values are introduced into the model as continuous area sources for the full three-hour simulation duration. This scenario enables evaluation of

how diesel pollutants and heat propagate within the airflow, how well they are diluted by the ventilation system, and where recirculation or localized buildup may occur.

### 3.3.4 Simulation Parameters and Configuration

To ensure physical realism in modeling airflow, thermal dynamics, and contaminant transport, the simulation framework was calibrated using representative thermodynamic and ventilation parameters consistent with mechanized room and pillar mining environments. These parameters were selected based on published empirical studies and refined to reflect expected underground operating conditions, with emphasis on air density, resistance coefficients, and gas dispersion under transient emission loads. All airflow resistance values were derived using Atkinson’s equation, and fan performance characteristics were defined using manufacturer-supplied pressure–flow curves.

The mine depth was set to 263 meters, corresponding to an atmospheric pressure of approximately 98.4 kPa. Ambient air temperature was initialized at 22°C, and relative humidity was fixed at 65%—values commonly recorded in deep underground coal and metal mines (Menéndez et al., 2022). The thermal conductivity of surrounding rock was modeled at 2.5 W/m·K, enabling simulation of heat exchange between mine walls and airflow. Gas transport was treated as passive dispersion without active chemical reactions or absorption dynamics. A summary of the key physical and environmental simulation parameters is presented in Table 2.

**Table 2. Key environmental and ventilation parameters used in the simulation.**

Parameter	Value	Description
Initial Air Temperature	22°C	Baseline air temperature for all ventilation and dispersion simulations
Relative Humidity	65%	Typical ambient humidity level in deep underground mines
Mine Depth	263 meters	Used to approximate subsurface barometric conditions

Atmospheric Pressure	98.4 kPa	Calculated from mine depth based on standard atmospheric lapse rate assumptions
Rock Thermal Conductivity	2.5 W/m·K	Controls heat exchange with adjacent rock strata (Menéndez et al., 2022)
Airway Friction Factors	0.015–0.025 Ns <sup>2</sup> /m <sup>4</sup>	Defined using Ventsim defaults, calibrated for resistance matching

Contaminant behavior in the simulation is modeled using passive scalar dispersion, assuming no chemical reactivity interactions with the surrounding rock surfaces. This approach allows for isolated analysis of gas transport dynamics based solely on ventilation-induced advection and diffusion. Heat exchange between the ventilation air and mine walls is computed through combined convective and conductive processes, utilizing Ventsim’s built-in thermal modeling capabilities. Emission sources—including both exposure-related gas surges and diesel particulate outputs—are triggered manually at predetermined locations and time steps to maintain consistency across scenario replications and ensure controlled comparative analysis.

### ***3.3.5 Performance Monitoring and Output Variables***

To replicate realistic atmospheric conditions within underground mining environments, the simulation focused on four key airborne contaminants: methane, nitrogen dioxide, carbon monoxide, and diesel particulate matter (DPM). These pollutants were selected based on their high prevalence in both post-exposure events and diesel-equipment-intensive operations, as well as their critical toxicological impact and regulatory significance. The inclusion of these gases facilitates a comprehensive evaluation of ventilation network performance under transient and sustained contaminant scenarios.

Methane was introduced at a concentration of 0.8%, representing a typical post-exposure accumulation level that remains safely below the lower explosive limit (LEL) of 5%. This value reflects commonly observed concentrations resulting from gas liberation in fractured strata and gob areas (Karacan et al., 2011). Although sub-explosive, such levels pose a ventilation challenge due to the gas’s flammability and buoyant dispersion profile.

Nitrogen dioxide was set at 3.0 ppm, approximating peak exposures produced by ANFO detonation byproducts and diesel engine exhaust. This concentration exceeds the NIOSH recommended Time-Weighted Average (TWA) threshold of 1.0 ppm and approaches the Short-Term Exposure Limit (STEL) of 5.0 ppm, justifying its inclusion as a critical hazard indicator (Fan & Xu, 2021). As a dense and highly irritant gas,  $NO_2$  tends to persist in low-velocity zones, particularly in inadequately ventilated crosscuts and dead ends.

Carbon monoxide was modeled at 30 ppm, representing a post-exposure average in confined drifts with incomplete combustion. While this value remains under the NIOSH TWA of 35 ppm and is well below the STEL of 200 ppm, it replicates a plausible scenario of chronic exposure in ventilation-deprived regions (Zhou et al., 2020). The concentration level selected enables assessment of long-duration inhalation risks and residual gas clearance capabilities.

Diesel particulate matter was simulated at a concentration of 350  $\mu\text{g}/\text{m}^3$ , corresponding to peak emissions from actively operating LHD equipment. This level significantly exceeds the MSHA occupational guideline of 160  $\mu\text{g}/\text{m}^3$ , providing a conservative benchmark for evaluating respiratory exposure risks and air quality degradation in diesel-intensive headings (Tutak et al., 2024).

The rationale, concentration thresholds, and regulatory context for each of these four contaminants are summarized in Table 3. All emissions were introduced as either instantaneous or continuous point sources within the  $CH_4$  exposure face and diesel zones, depending on the operational scenario. Five strategically positioned sensor nodes were used to capture pollutant concentration trends, clearance durations, and spatial migration across the modeled airways. Output variables were benchmarked against occupational exposure limits and Ventsim-derived airflow metrics to determine the ventilation system’s capacity to contain and dissipate contaminant loads.

**Table 3. Input variables used in the simulation.**

Contaminant Gas	Input variables	Units	Rationale	References
Methane ( $CH_4$ )	0.8	%	Represents elevated post-exposure level,	Karacan et al. (2011)

			below explosive limit (LEL ~5%)	
Nitrogen Dioxide ( $NO_2$ )	3.0	ppm	Common concentration from ANFO exposure and diesel engines; exceeds NIOSH TWA (1 ppm)	Fan and Xu (2021)
Carbon Monoxide ( $CO$ )	30	ppm	Reflects average levels post-exposure; below NIOSH TWA (35 ppm), suitable for prolonged hazard modeling	Zhou et al. (2020)
Diesel Particulate Matter (DPM)	350	$\mu\text{g}/\text{m}^3$	Based on typical LHD operation range (100–500 $\mu\text{g}/\text{m}^3$ ); above OSHA reference value (~160 $\mu\text{g}/\text{m}^3$ )	Tutak et al. (2024)

Regulatory reference limits for gas exposure were derived from the standards established by the Occupational Safety and Health Administration (OSHA), the National Institute for Occupational Safety and Health (NIOSH), and the Mine Safety and Health Administration (MSHA). Specifically, the permissible Time-Weighted Average (TWA) for carbon monoxide ( $CO$ ) is set at 50 ppm, the ceiling limit for nitrogen dioxide ( $NO_2$ ) is 5 ppm, and the DPM reference value is defined by MSHA at 160  $\mu\text{g}/\text{m}^3$ . These thresholds served as evaluation benchmarks throughout the simulation process. By comparing temporal concentration profiles across the three modeled scenarios—baseline, post-exposure, and diesel-intensive operations—this study enables a quantitative assessment of the ventilation system’s ability to maintain contaminant levels below regulatory exposure limits. Such analysis provides critical insights into the network’s

capacity to mitigate both localized surges and broader accumulations of airborne toxicants under realistic underground operating conditions.

### **3.4 Simulation Workflow and Procedure**

The simulation process undertaken in this study followed a rigorously structured workflow to ensure consistency, transparency, and reproducibility across all modeled scenarios. All simulations were performed using Ventsim Visual™, leveraging its capacity for dynamic airflow modeling, contaminant transport, and heat dispersion within complex underground environments. Rather than treating each scenario independently, a sequential simulation strategy was adopted, wherein baseline calibration informed all subsequent emission-based analyses. Intake and return airways were assigned at opposite sides of the model, and ventilation flow was driven using a booster fan with a fixed capacity of 181 m<sup>3</sup>/s.

Friction factors were assigned based on Atkinson resistance values, ranging from 0.015 to 0.025 Ns<sup>2</sup>/m<sup>4</sup>, calibrated to reflect typical mine tunnel roughness (Menéndez et al., 2022). The simulation first ran under a steady-state configuration to establish baseline airflow performance, ensuring that airflow velocities exceeded 0.5 m/s in all production headings and that volumetric distribution remained balanced across the network. Mass balance and vector field stability were used to confirm calibration integrity.

Following the baseline validation, emission sources were sequentially introduced for each operational scenario. In Scenario 2, post-exposure conditions were modeled by injecting 250 ppm CO, 80 ppm NO<sub>2</sub>, and 0.8% CH<sub>4</sub> at the northeastern exposure face, representing an instantaneous point-source release within a 30-meter radius (Ge et al., 2024; Huang et al., 2025; Karacan et al., 2011). Scenario 3 introduced continuous emissions from two diesel LHD units located in central and southern drifts, each emitting 50 ppm CO, 350 µg/m<sup>3</sup> DPM, 3.0 ppm NO<sub>2</sub>, and producing a thermal output of 7.5 kW per unit (Fan & Xu, 2021; Kumar et al., 2013; Tutak et al., 2024).

Ambient environmental conditions were defined to reflect deep underground settings: ambient temperature was fixed at 22°C, rock thermal conductivity at 2.5 W/m·K, relative humidity at 65%, and barometric pressure at 98.4 kPa, simulating a depth of approximately 263 meters. Gas transport was treated as passive scalar dispersion without

reactive interactions, and heat exchange was modeled via convective and conductive transfer between air and rock walls.

Simulations were executed over different time periods to capture peak point and stabilization times. Output variables—including  $CH_4$ ,  $CO$ ,  $NO_2$  and DPM, airflow velocity, and dry bulb temperature—were recorded at six sensor nodes strategically positioned along a single entry of working face. These nodes provided spatial coverage of intake, return, central, and emission-intensive regions.

To ensure physical validity and numerical stability, all simulation outputs underwent quality control. Anomalous readings such as negative velocities or concentration spikes were identified and corrected via boundary condition refinement. Key results—including gas concentration time-series, velocity vector maps, and isothermal overlays—were exported for inter-scenario comparison and regulatory benchmarking.

Evaluation was conducted against exposure standards defined by OSHA, NIOSH, and MSHA, including 50 ppm TWA for  $CO$ , 5 ppm ceiling for  $NO_2$ ,  $160 \mu\text{g}/\text{m}^3$  for DPM, and an explosive threshold of 5% for  $CH_4$ . These comparisons supported quantitative assessments of ventilation performance under realistic and stress-induced operational conditions (Asfaw et al., 2013; Olczak et al., 2023; Tutak et al., 2024).

### **3.5 Evaluation Metrics and Output Analysis**

The assessment of ventilation performance and contaminant dispersion in the simulated room and pillar mine layout was based on a multi-dimensional evaluation framework. This framework was developed to reflect occupational safety regulations, ventilation engineering best practices, and empirical standards from prior simulation-based studies. The primary objective of the output analysis was to quantify the ventilation network's effectiveness in diluting, transporting, and clearing hazardous airborne contaminants from critical operational zones over time.

The key pollutants under examination—methane ( $CH_4$ ), nitrogen dioxide ( $NO_2$ ), carbon monoxide ( $CO$ ) and diesel particulate matter (DPM)—were monitored at six sensor monitors (Table 1) strategically placed throughout the model, including the intake and return airways, the exposure face, the central junction, and the diesel loading zone.

For each contaminant, temporal concentration profiles were generated across a three-hour dynamic simulation window, capturing both the transient peaks and decay behavior at each monitoring location.

Regulatory exposure thresholds were used as comparative benchmarks: 50 ppm for CO (TWA), 5 ppm ceiling limit for  $NO_2$ , and  $160 \mu\text{g}/\text{m}^3$  for DPM, as defined by the Occupational Safety and Health Administration (OSHA) and Mine Safety and Health Administration (MSHA) guidelines (Asfaw et al., 2013; Olczak et al., 2023). Methane concentrations were interpreted in relation to its lower explosive limit (LEL) of approximately 5%, with the simulated value of 0.8% representing a critical pre-flammability threshold (Karacan et al., 2011).

Primary evaluation metrics included:

1. **Peak Concentration Values:** The highest concentration of each contaminant recorded at any sensor node during the simulation period.
2. **Time-to-Threshold Clearance:** The duration required for pollutant concentrations to fall below regulatory limits following emission events, particularly for CO,  $NO_2$ , and DPM.
3. **Airflow Velocity Distribution:** Vector field outputs from Ventsim were analyzed to map air movement across the entire simulated network. Particular focus was placed on identifying areas with velocity drops below 0.3 m/s—indicative of potential stagnation zones (Wu et al., 2022).
4. **Thermal Gradients and Stratification Risks:** For scenarios involving diesel operation, temperature deviations above  $2^\circ\text{C}$  from ambient were flagged as critical, with isothermal maps used to evaluate whether localized heating led to altered airflow patterns or stratification. These thermal anomalies were further cross-referenced with concentration peaks to assess interactive dispersion effects (Fan & Xu, 2021).
5. **Composite Multi-Parameter Analysis:** Overlays of concentration, velocity, and temperature data were generated to visualize the interaction between pollutant transport and thermal-induced airflow modification. This allowed for the identification of compound risk areas, especially under dual-source emission scenarios.

Supplementary indicators included:

1. **Spatial Coverage Efficiency:** The number of monitoring nodes detecting concentrations above threshold limits at any point in time, used to assess spatial extent of contamination.
2. **Standard Deviation and Variability:** Statistical measures were applied to determine the dispersion consistency of each gas across monitored points and simulation intervals.
3. **Mass Balance and Flow Continuity Checks:** As no empirical calibration was conducted, internal validation included confirmation of consistent inflow and outflow air volumes, symmetrical pollutant decay along mirrored geometries, and uniform clearance profiles in zones with comparable ventilation input.

Results from this analytical framework are presented through tabulated summaries, dynamic simulation plots, and velocity vector maps in Chapter 4. These outputs form the foundation for cross-scenario comparison and guide the interpretive discussion in Chapter 5. By correlating clearance times, airflow stagnation, and gas persistence, the model enables the identification of structural ventilation weaknesses and supports design-oriented recommendations for hazard mitigation in underground mining operations.

### **3.6 The use of Ventsim and @Risk Softwares**

The Ventsim software is used for conducting simulations of ventilation in the given design. It simulates the changes in temperature, airflow velocity, airflow quantity, pressure and so on in the mine. The software uses CFD to simulate the movement of airflow. Meanwhile, @Risk Palisade is used to compute risk analysis in decision-making. It is based on Monte Carlo simulations and provides different types of distributions to assess the probability. In the case of this case-study, it computed exposure volume by considering multiple input variables. Also, it assisted with making comparisons between proven distributions like a lognormal.

## 4. RESULTS

### 4.1 Evaluation Metrics and Output Analysis

The baseline simulation was conducted to establish reference conditions for airflow dynamics and environmental stability in the absence of contaminant sources. The modeled geometry represented a simplified room-and-pillar section of an underground mine, approximately 4644 meters in length and 1140 meters in width. Due to the dimensions of this model, only part was simulated to keep computational efficiency at the same time as to preserve key spatial features commonly found in production-level mining. The simulation domain was configured with a fixed forced ventilation setup, wherein a main fan delivering 181 m<sup>3</sup>/s of airflow introduced fresh air from the western intake drift and exhausted return air through the easternmost airway. To capture the topographical context and spatial behavior of the simulated airflow, both top-down and oblique perspectives of the mine model were generated. These visualizations supported qualitative assessment of airflow trajectories and helped validate model symmetry. Six dynamic monitors were placed along the working face system to monitor baseline velocities and environmental parameters prior to the introduction of emission events. Figures 1-5 illustrate the mine layout and topographic visualization outputs derived from Ventsim Visual™.

The total length of the airways is 110,479 m, the number of airways is 3105, fan pressure simulation type is total pressure method, and network efficiency is 63.9% as could be seen in Figure 6.

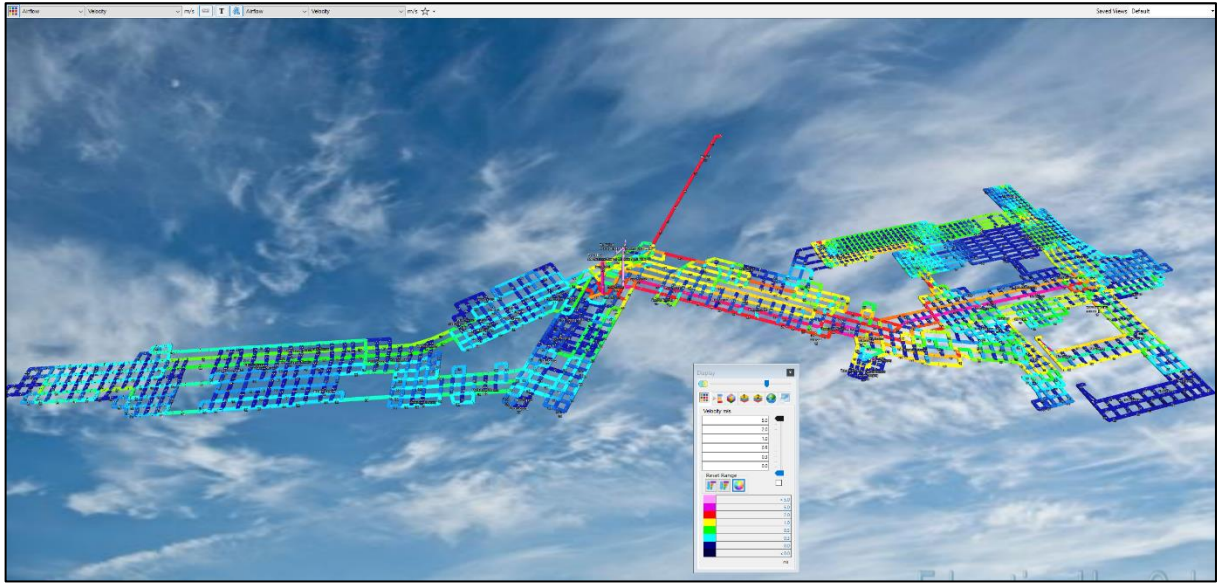


**Figure 1. The Scheme of the Room & Pillar mining system.**

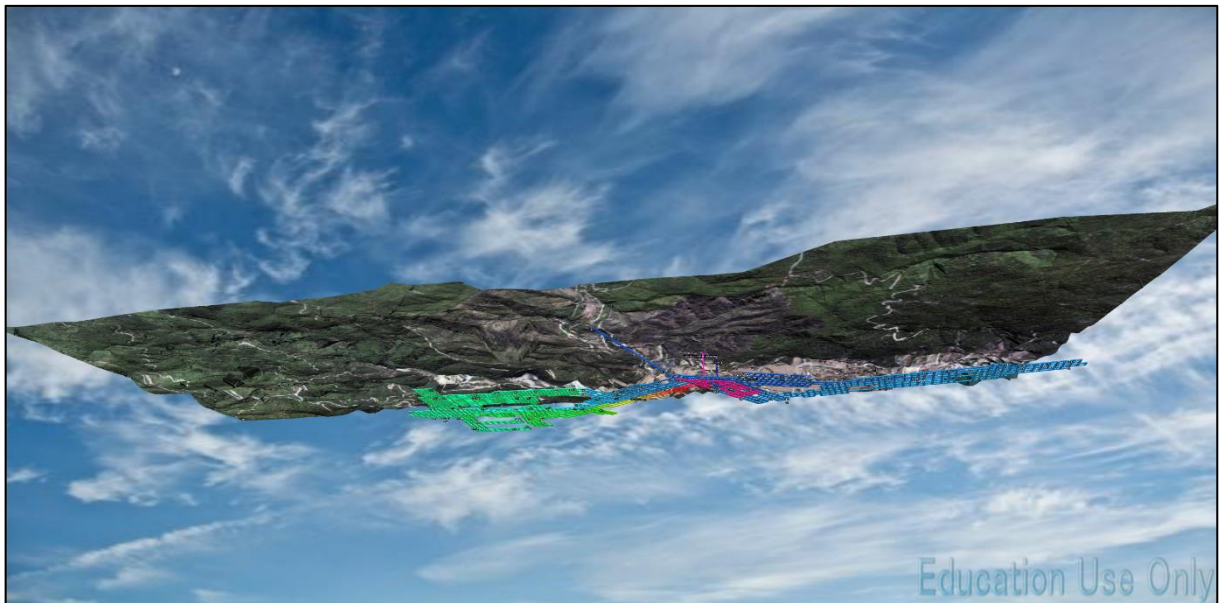


**Figure 2. The view on the Topography and the mine layout.**

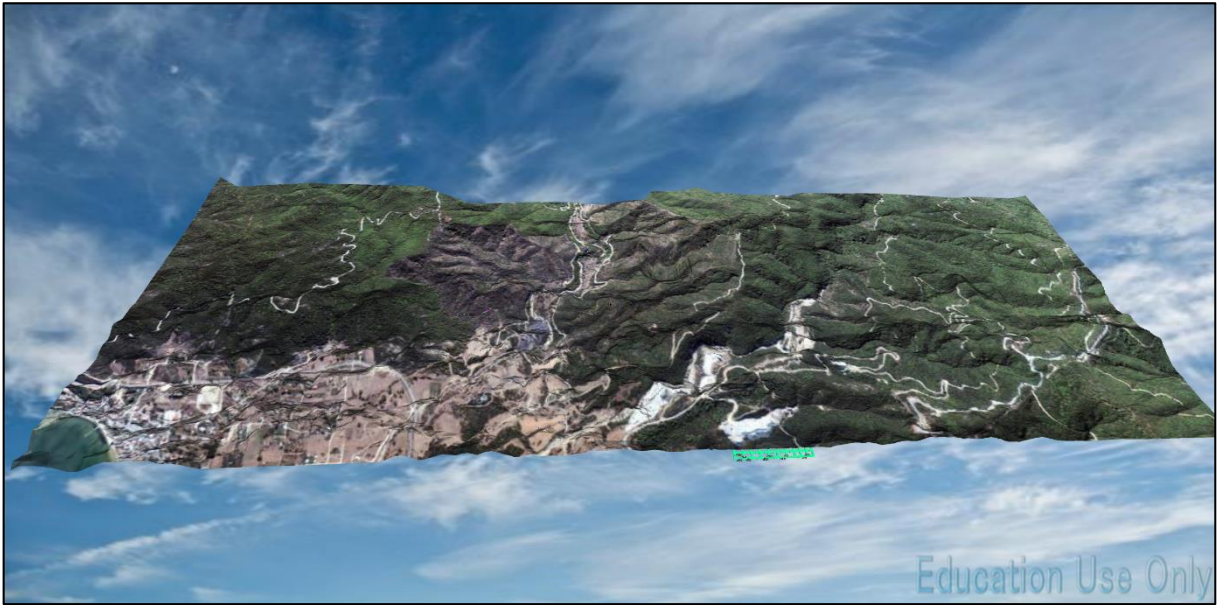


**Figure 3. The view on the Topography.**

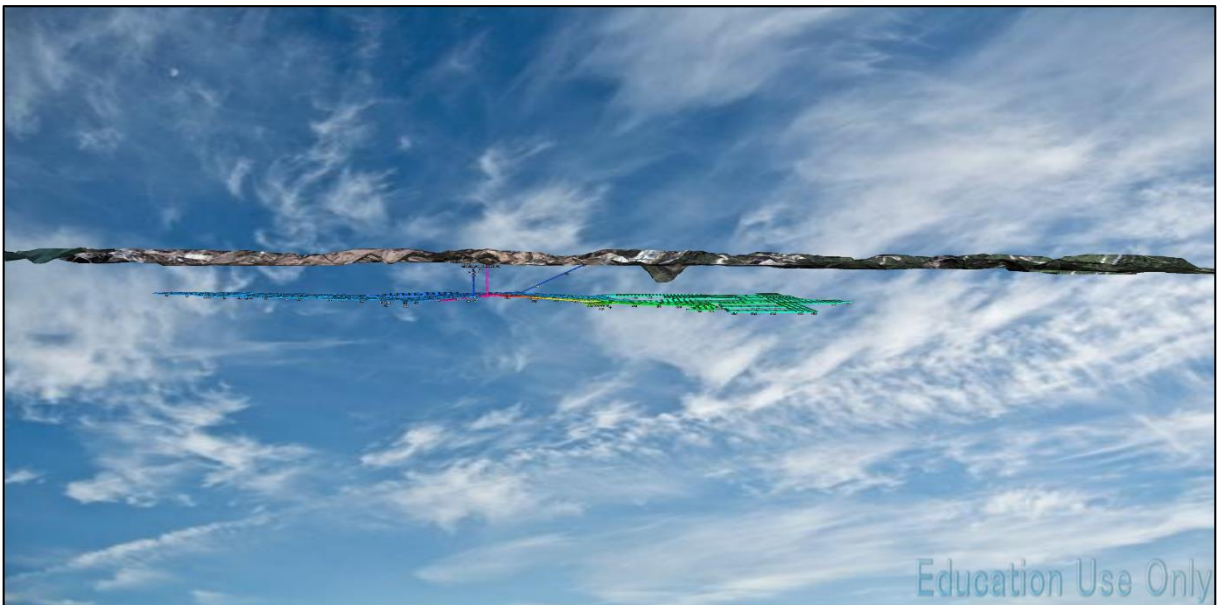


**Figure 4. The view on the Topography from the side / Horizontal View of the Topography.**

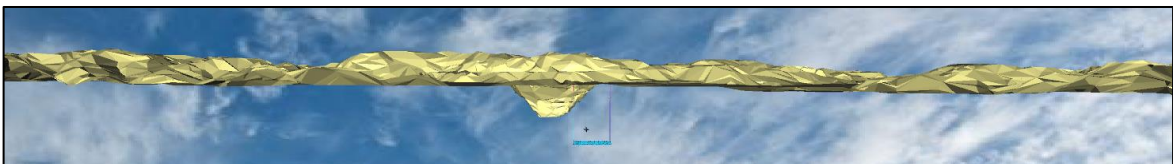


**Figure 5. Oblique topographic rendering highlighting overburden conditions.**

NETWORK SYSTEM SUMMARY	
<b>Example Coal Mine - Press 'X' to hide surfaces</b>	
Compressible Airflows	No
Natural Ventilation Pressure	No
Fan Pressure Simulation Type	Total Pressure Method
Stage	0: Stage 1
Airways	3105
Current Stage Segments	2923
Total length	110,478.8 m
Total airflow intake	181.2 m <sup>3</sup> /s
Total airflow exhaust	181.2 m <sup>3</sup> /s
Total massflow	217.44 kg/s
Mine resistance (excluding duct)	0.04480 Ns <sup>2</sup> /m <sup>8</sup>
Mine resistance (including duct)	0.04480 Ns <sup>2</sup> /m <sup>8</sup>
<b>POWER SUMMARY</b>	
AIR (friction loss) Power	266.5 kW Total
	39.3 kW Shaft
	227.2 kW Drive
	0.0 kW Vent Duct
Refrigeration Power Input	0.0 kW
<b>INPUT Power Electrical</b>	<b>417.3 kW</b>
<b>Network Annual Power Cost</b>	<b>\$ 365,535</b>
<b>Network Efficiency</b>	<b>63.9 %</b>

**Figure 6. Baseline Ventilation Network System Summary.**

Under steady-state conditions, airflow velocities exhibited a robust and balanced distribution across the newly modeled ventilation network. The total airflow intake and exhaust rates were matched at 181.2 m<sup>3</sup>/s, resulting in a mass flow of 217.44 kg/s through the 110,478.9-meter airway system. Air velocity distribution varied across the layout, with higher velocities—up to 5.0 m/s—observed in the main intake and return shafts, while peripheral or isolated headings showed reduced flow velocities below 1.0 m/s, especially in non-productive blind entries. These ventilation conditions are within industry-recommended thresholds for room-and-pillar mining operations and are well-suited to support diesel-powered machinery (Krause & Krzemień, 2014).

Network resistance values of 0.04480 Ns<sup>2</sup>/m<sup>8</sup> indicate a moderate airflow impedance, consistent with a system composed of rectangular headings and unlined rock surfaces. The system operated with a total fan power of 417.3 kW distributed across two fans, achieving a network efficiency of 63.9% and an estimated annual power cost of \$365,535. These energy performance metrics reflect typical operational ranges for mid-scale ventilation systems using fixed booster fans. Spatial flow heterogeneity and localized constrictions were identified, which may act as potential accumulation points under dynamic emission conditions.

Figure 7 visualizes the airflow velocity distribution simulated in Ventsim Visual™, highlighting key features such as velocity gradients, minor eddies, and areas of

reduced flow efficiency. These observations will inform subsequent scenario analyses involving gas dispersion and ventilation response to emission events.



**Figure 7. Airflow velocity field (Baseline Scenario).**

Thermal and humidity conditions remained spatially consistent across the simulated ventilation network during the baseline scenario. The initial air temperature was maintained at 22.5°C, with a constant relative humidity of 65%, replicating typical underground mine environments in temperate climatic regions under non-operational conditions. In the absence of  $CH_4$  exposure, diesel equipment, or geothermal heat flux, no evidence of thermal stratification or convective anomalies was observed over the 180-minute simulation duration.

As no emission sources were activated in this scenario, contaminant concentrations at all five designated monitoring nodes remained at zero for carbon monoxide (CO), nitrogen dioxide ( $NO_2$ ), methane ( $CH_4$ ), and diesel particulate matter (DPM). This confirms the fidelity of the clean-air benchmark simulation and establishes a reference condition for comparative analysis against subsequent emission-intense scenarios.

Absolute Pressure across the model ranged from 99.7 Pa at the intake zone to approximately 101 Pa at the return airway, relative to the ambient atmospheric pressure of 98.4 kPa. These differentials are indicative of a functional forced ventilation system, wherein negative values correspond to low-pressure suction zones that facilitate exhaust

flow. Such pressure profiles align with established theoretical models of subsurface airflow behavior and are typical of extended room and pillar layouts characterized by moderate to high airway resistance (McPherson, 1993). The spatial distribution of static pressure across the entire circuit is illustrated in Figure 8.

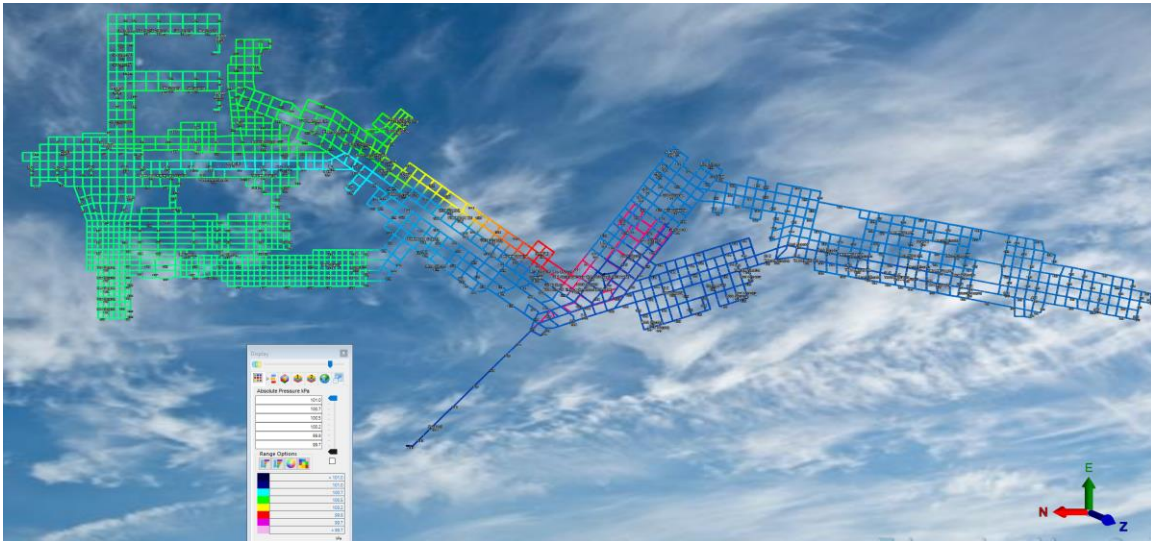


**Figure 8. Static Pressure Distribution in the Mine Ventilation Network (Baseline Scenario).**

Baseline scenario suggests that the case of absence of toxic gases should be considered too and  $CH_4$  concentrations were chosen in order to show the case of absence of toxic gas, which could be seen in Figure 9.

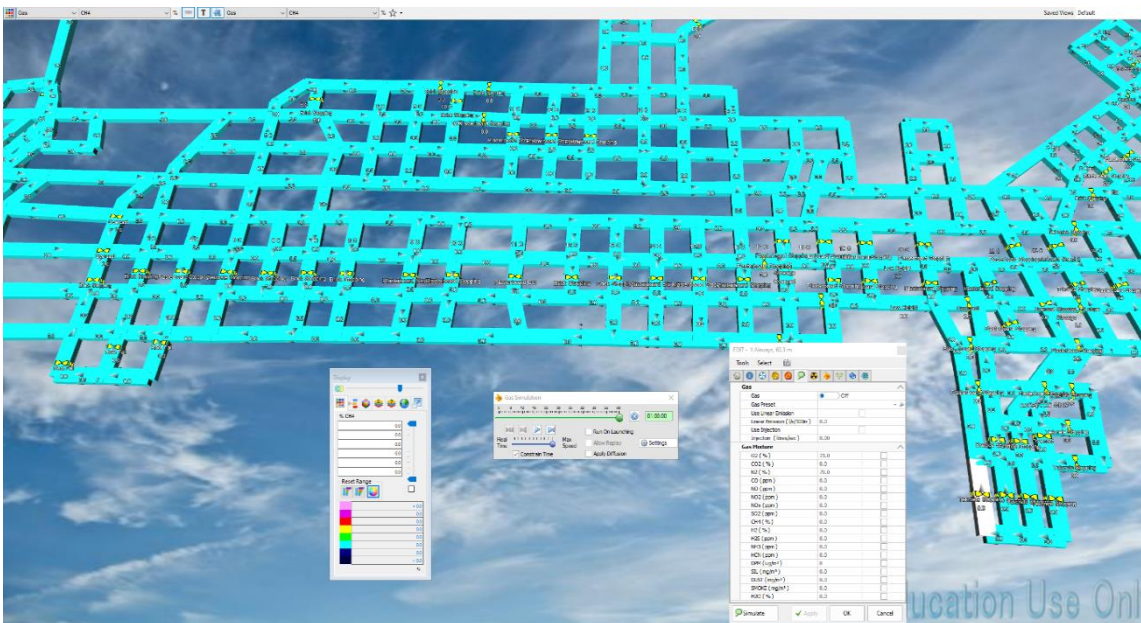


**Figure 9. Initial dynamic simulation without  $CH_4$ .**

## 4.2 Post-Exposure Gas Dispersion Results

This section presents the simulation results of gas dispersion dynamics following a controlled exposure event and concurrent diesel equipment operation within the modeled underground mine section. The exposure scenario replicates a short-term, high-intensity release of carbon monoxide (CO), nitrogen dioxide ( $NO_2$ ), and methane ( $CH_4$ ) from the designated detonation site at Crosscut 1, lasting three minutes. Simultaneously, diesel load-haul-dump (LHD) equipment was simulated in adjacent headings, contributing to additional emissions of CO and  $NO_2$  under continuous operation.

Ventilation behavior during this phase remained aligned with the steady-state airflow characteristics established in Section 4.1. Directional integrity and airflow velocity distribution were preserved across the entire model domain. Pollutant transport was evaluated at five spatially distributed sensor locations, capturing transient peak concentrations and tracking their clearance over a 180-minute simulation period.

Table 4 consolidates the maximum recorded values for  $CH_4$ , CO, and  $NO_2$  at each monitoring point, along with the time required for each gas to fall below regulatory or operational safety thresholds: 0.8% for  $CH_4$  (to ensure operation below the lower explosive limit), 50 ppm for CO (OSHA TWA), and 3 ppm for  $NO_2$  (adjusted ceiling limit based on acute exposure considerations). This unified table structure allows for direct comparison of contaminant behavior across gases and ventilation zones, supporting the assessment of localized airflow performance and hazard clearance efficiency under realistic multi-source emission conditions.

**Table 4. Summary of gas Concentrations Following Methane Gases Exposure Event.**

Monitoring Point	Max CO (ppm)	Max $CH_4$ (%)	Max $NO_2$ (ppm)	Time to CO <25 ppm (min)	Time to $NO_2$ <3 ppm (min)	Time to $CH_4$ <0.8 % (min)
Intake Airway Node	29.8	0.8	3.0	10	8	6
Return Airway Node	20.3	0.5	2.0	24	18	12
Face Node	7.4	0.2	0.7	30	24	16

LHD Zone Nodes	22.1	0.6	2.2	27	20	14
Mid-Point Junction Node	22.7	0.6	2.3	28	21	15

Dynamic simulation snapshots were captured at different time intervals to account for the varying rise times in explosion and stabilization for each exposure event. This approach helped evaluate the temporal and spatial evolution of toxic gas dispersion within the simulated room-and-pillar mine ventilation system.

The simulations specifically focused on the detonation zone at Monitor #1, where  $CH_4$ ,  $CO$  and  $NO_2$  were released simultaneously. The gas dispersion was tracked using six dynamic monitors distributed along Entry 1 (see Figure 10).

Figure 10 shows zero values for  $CH_4$  gas in the initial state, prior to any simulations taking place.

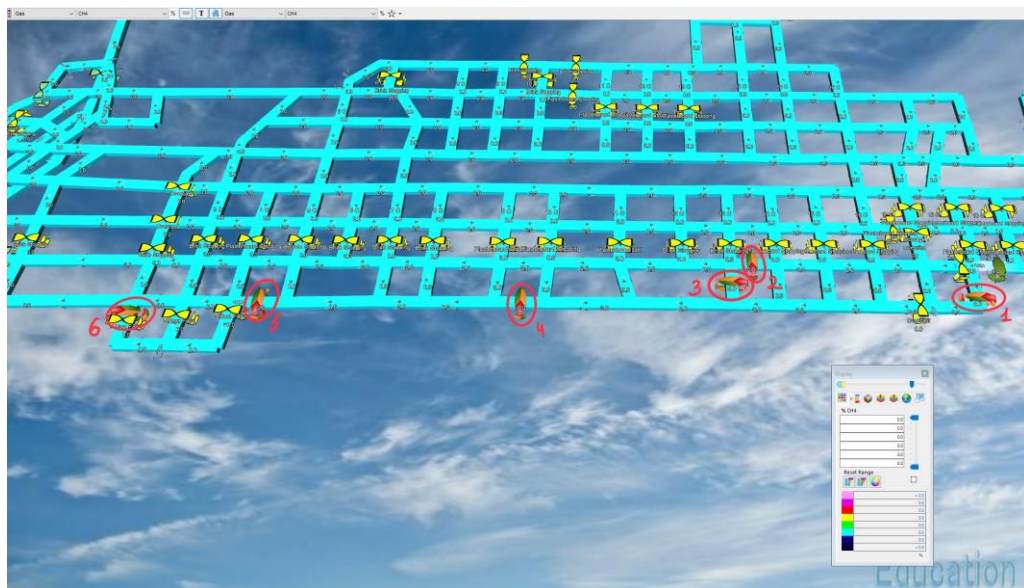


**Figure 10. Dynamic monitor's locations.**

In the Figure 11, the  $CH_4$  percentage starts from nearly zero, and within less than 30 seconds, it shows a sudden and steep increase. The detection quickly stabilizes at around 0.8%, rapid detection suggests a high sensitivity of the sensor as it was very near to the explosion point, 50 meters away. In the Figure 2, the  $CH_4$  percentage starts from a 0 value and increases rapidly to 0.154% at approximately 2 minutes and after a little bit reaches a relatively stable level. There is a lower accumulation of methane gas compared to the first monitor although there is a stowage on the line which allows air to move easier.

At the 4<sup>th</sup> monitor, which is located nearly 435 meters away from the methane exposure site shows around 0.6% of  $CH_4$  gas slightly after 3 minutes. It can be explained by the fact that the detector located further than the first detector for about 385 meters. In the Figure 15, the  $CH_4$  detection at 650 meters away from the methane exposure site starts low but increases quickly slightly after 4 minutes till 0.58%, reaching a stable plateau of 0.6% after approximately 4 minutes. The 6<sup>th</sup> monitor shows a delayed increase in  $CH_4$  percentage, with the rise happening after around 7 minutes. The  $CH_4$  level then stabilizes around 0.6% after 1 hour. It may happen due to the fact that the detector is located at the turns, which cause friction and its distance from the methane exposure site for 765 meters.

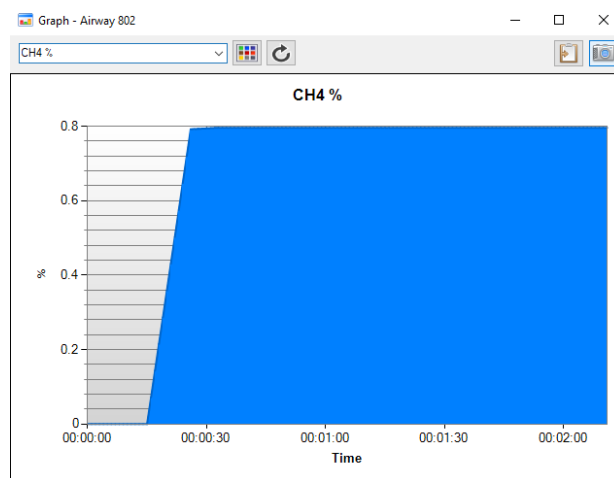


**Figure 11. Dynamic Simulation of  $CH_4$  gas at 3 Minutes Post-Exposure at the 1<sup>st</sup> monitor.**

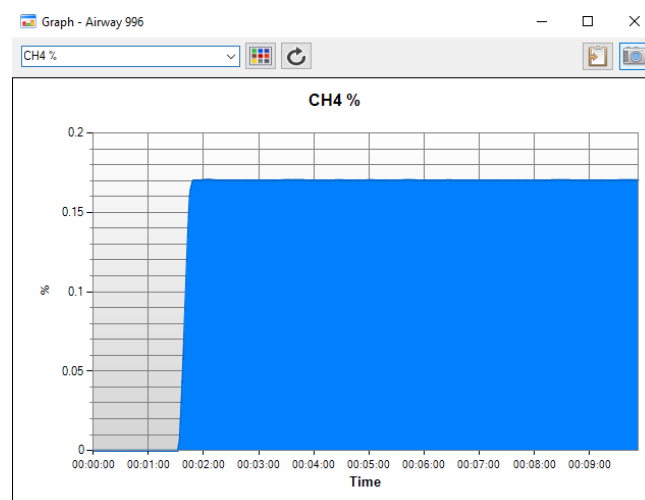


**Figure 12. Dynamic Simulation of  $CH_4$  gas at 10 Minutes Post-Exposure at the 2<sup>nd</sup> monitor.**

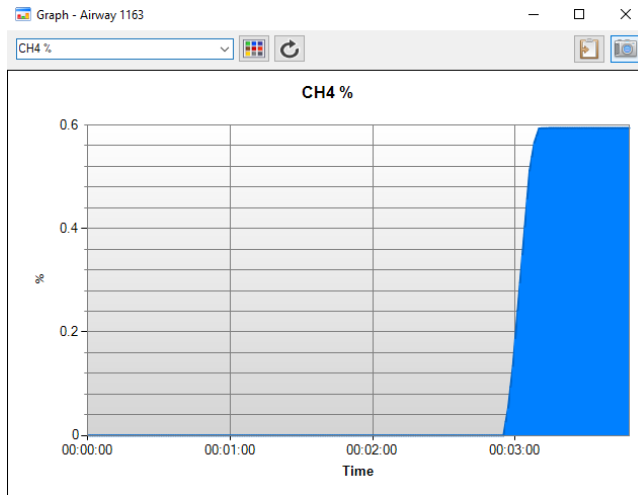


**Figure 13. Dynamic Simulation of CH4 gas at 4 Minutes Post- Exposure at the 4<sup>th</sup> monitor.**

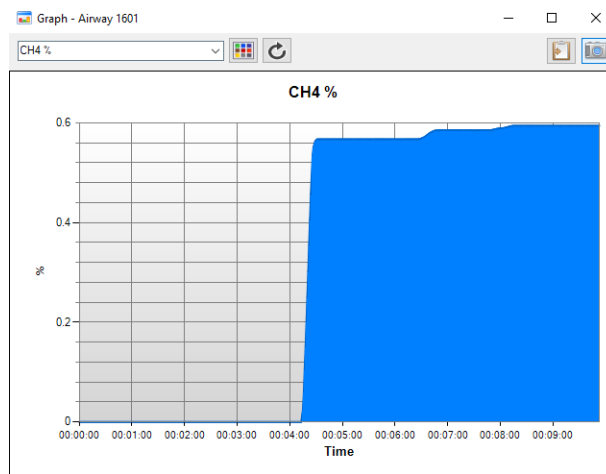


**Figure 14. Dynamic Simulation of CH4 gas at 10 Minutes Post- Exposure at the 5<sup>th</sup> monitor.**

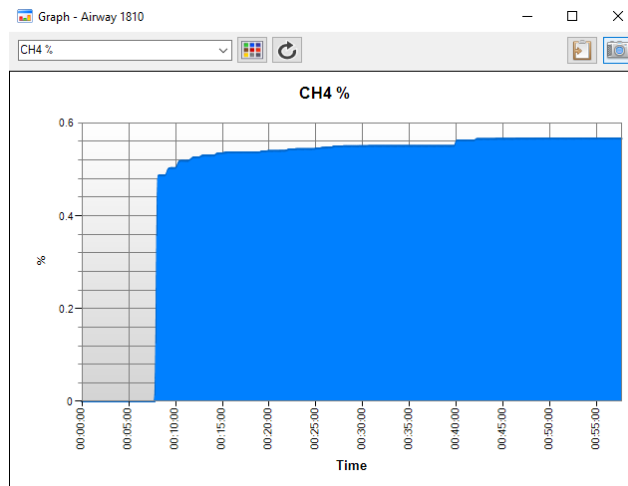


**Figure 15. Dynamic Simulation of CH4 gas at 60 Minutes Post- Exposure at the 6<sup>th</sup> monitor.**

The simulation of  $NO_2$  gas exhibited a similar pattern of gas concentrations across the monitors as  $CH_4$ , which can be attributed to the use of the same detectors. Figure 16 shows the results from a 2-minute simulation, during which  $NO_2$  peaked at 3 ppm within

approximately 25 seconds and then remained constant. The second monitor displayed a gradual increase in gas concentration, reaching 0.64 ppm between 1:30 and 2 minutes. The third detector reached its first peak of 0.56 ppm just after 5 minutes, followed by a second peak of 0.64 ppm, after which it stabilized. Monitors 4 to 6 exhibited similar patterns, with fluctuating values before stabilizing. The fourth monitor reached its first peak of 2.2 ppm at the 2nd minute and remained steady at 2.4 ppm after 20 minutes. Similarly, monitor #3 recorded its first peak of 2.1 ppm at the 4th minute, stabilizing at 2.3 ppm after approximately 23 minutes. These variations can be explained by factors such as friction and distance, which affect the timing of gas detection and their distribution over time.

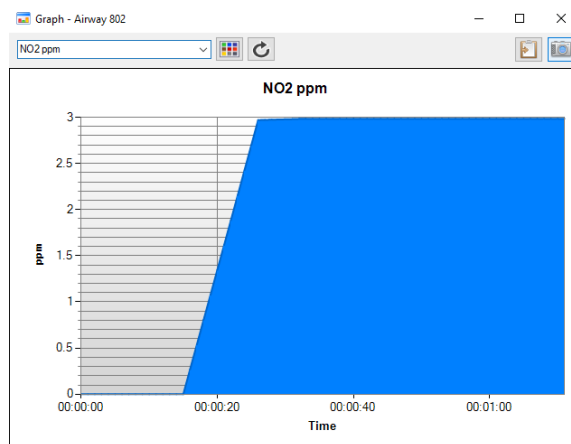


**Figure 16. Dynamic Simulation of NO2 gas at 2 Minutes Post- Exposure at the 1<sup>st</sup> monitor.**

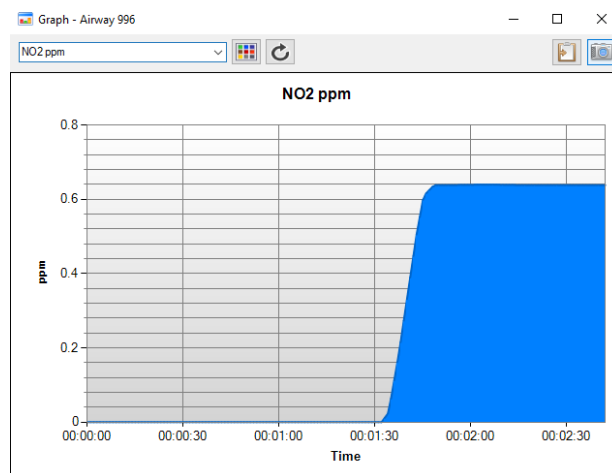


**Figure 17. Dynamic Simulation of NO2 gas at 3 Minutes Post- Exposure at the 2<sup>nd</sup> monitor.**

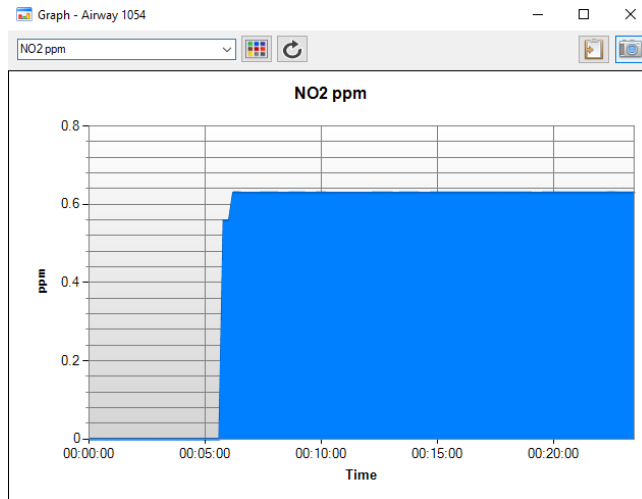


**Figure 18. Dynamic Simulation of NO2 gas at 25 Minutes Post- Exposure at the 3<sup>rd</sup> monitor.**

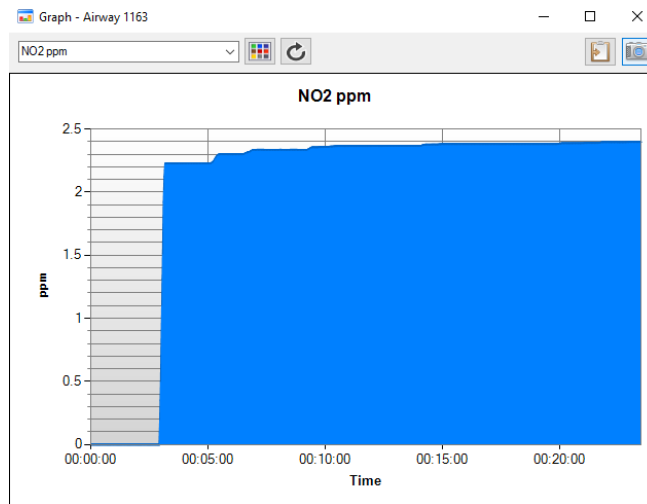


**Figure 19. Dynamic Simulation of NO2 gas at 23 Minutes Post- Exposure at the 4<sup>th</sup> monitor.**

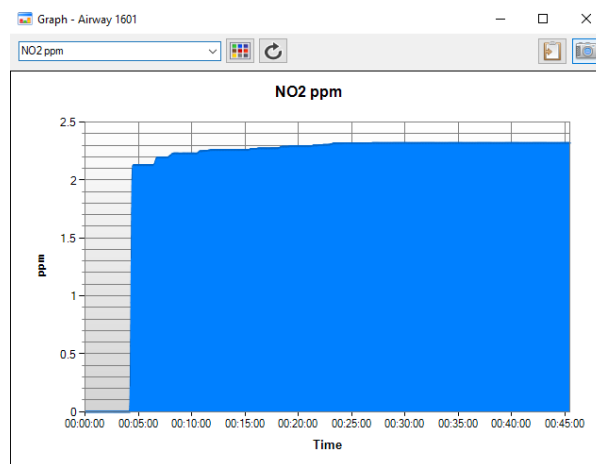


**Figure 20. Dynamic Simulation of NO2 gas at 45 Minutes Post- Exposure at the 5<sup>th</sup> monitor.**

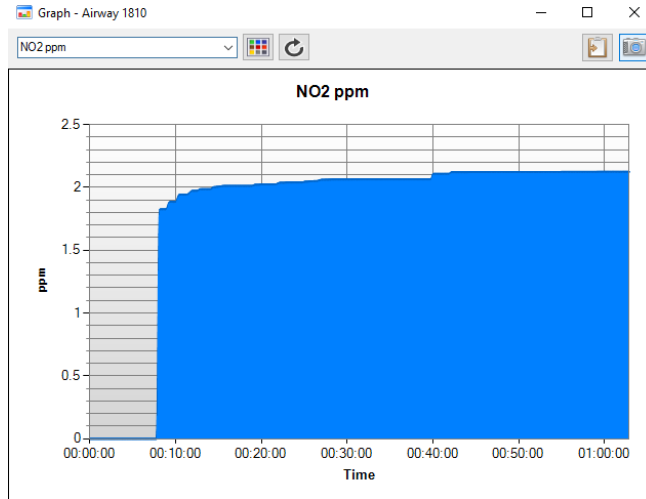


**Figure 21. Dynamic Simulation of NO<sub>2</sub> gas at 65 Minutes Post- Exposure at the 6<sup>th</sup> monitor.**

Carbon monoxide (CO) reached its peak on detection faster than methane ( $CH_4$ ), but slower than nitrogen oxide (NO<sub>2</sub>). All gases stabilize after reaching their respective peaks, but CO takes a bit longer to plateau compared to  $NO_2$  and  $CH_4$ , which stabilize more quickly. The other simulations show the similar pattern of distribution as  $NO_2$  and  $CH_4$ .

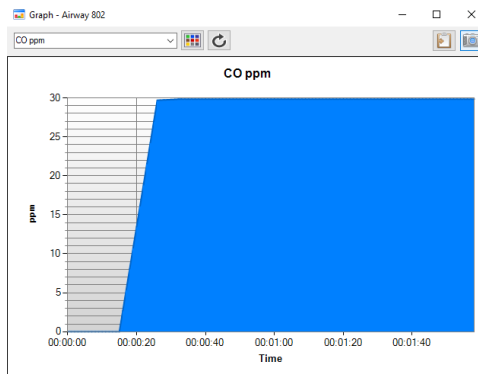


**Figure 22. Dynamic Simulation of CO gas at 2 Minutes Post- Exposure at the 1<sup>st</sup> monitor.**

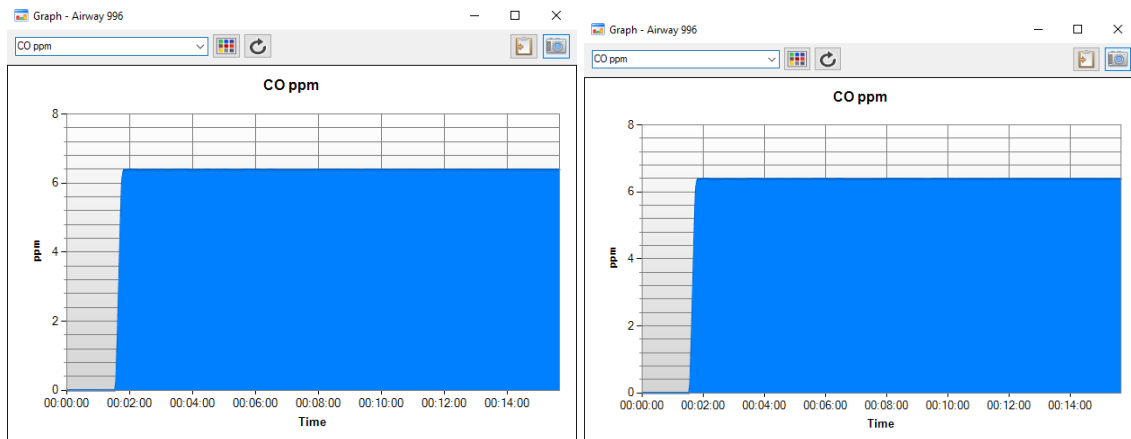


**Figure 23. Dynamic Simulation of CO gas at 15 Minutes Post- Exposure at the 2<sup>nd</sup> and 3<sup>rd</sup> monitors.**

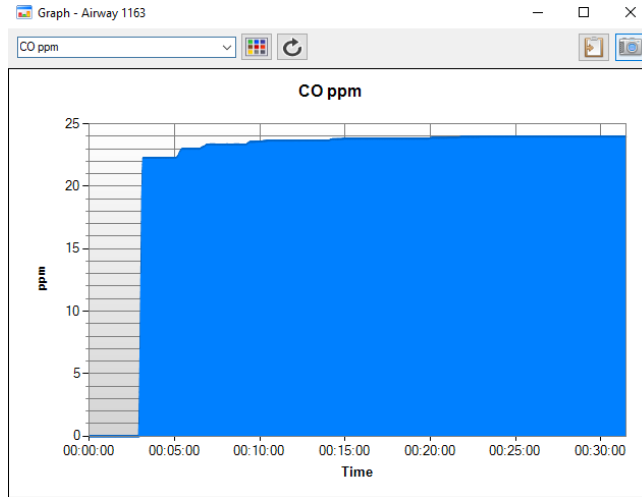


**Figure 24. Dynamic Simulation of CO gas at 35 Minutes Post- Exposure at the 4<sup>th</sup> monitor.**

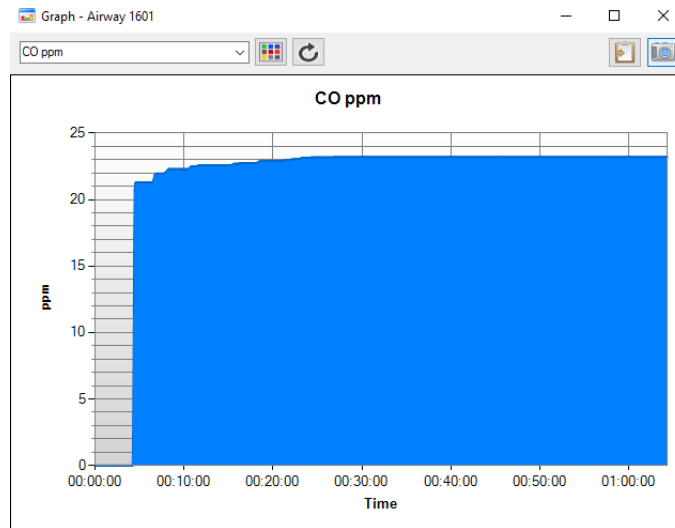


**Figure 25. Dynamic Simulation of CO gas at 65 Minutes Post- Exposure at the 5<sup>th</sup> monitor.**

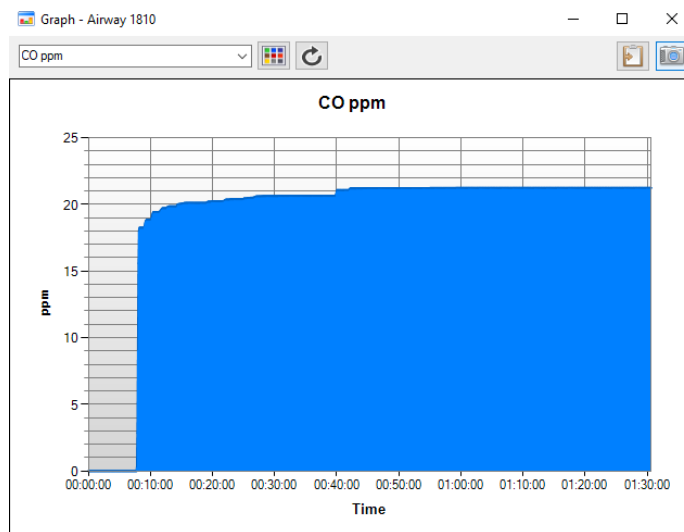


**Figure 26. Dynamic Simulation of CO gas at 90 Minutes Post- Exposure at the 6<sup>th</sup> monitor.**

### 4.3 Diesel Equipment Operation

This section presents the results of the dynamic simulation focused exclusively on diesel equipment operation, particularly the dispersion and persistence of diesel particulate matter (DPM) within the modeled underground mine layout.

Emission rates were derived from empirical studies of underground diesel fleets, with DPM released at a rate of 0.4 mg/s, representing combustion output from a 180 kW diesel engine (Tutak et al., 2024). The simulation was designed to reflect high-exposure conditions, modeling continuous engine operation without advanced filtration or emission suppression systems. Ambient airflow conditions, as established in the baseline scenario (Section 4.1), remained constant, with average ventilation velocities of approximately 3 m/s across primary headings.

As shown in Table 5, DPM concentrations peaked in the Intake Airway Node at 348  $\mu\text{g}/\text{m}^3$ , consistent with localized exposure at the emission source. Elevated values were also observed in the Mid-Point Junction Node (265  $\mu\text{g}/\text{m}^3$ ) and the Return Airway Node (237  $\mu\text{g}/\text{m}^3$ ), demonstrating pollutant migration into adjacent headings. The Exposure Face Node recorded a lower peak of 87  $\mu\text{g}/\text{m}^3$ , indicating that the pollutant has traveled a greater distance from the emission source. The LHD Zone Nodes reached a peak of 257  $\mu\text{g}/\text{m}^3$ , aligning with their role as the central point for ventilation and equipment operation.

Exposure durations were measured against the Mine Safety and Health Administration (MSHA) ceiling threshold of 350  $\mu\text{g}/\text{m}^3$ . The Intake Airway Node reported no exceedance, as expected from its role as a clean-air reference location. The Return Airway Node exceeded the threshold for 18 minutes, and the Exposure Face Node had an exceedance duration of 62 minutes. The Mid-Point Junction Node exceeded the threshold for 99 minutes, while the LHD Zone Nodes exceeded the threshold for 104 minutes, confirming extended exposure in the central and downstream ventilation zones.

These findings emphasize the persistence of DPM in central and downstream ventilation zones, even under adequate airflow conditions. The data suggest that equipment mobility and operational scheduling should be synchronized with localized ventilation design to minimize worker exposure to diesel particulates in confined airways.

The simulations showed that over a period of 35 minutes, DPM concentrations can circulate up to 250  $\mu\text{g}/\text{m}^3$  in the working face. These results confirm the need for proactive ventilation strategies in diesel-intensive mining operations, particularly in geometrically constrained room-and-pillar sections where particulate buildup may persist in operational hot zones.

**Table 5. Summary of DPM Concentrations during Diesel Equipment Operation at LHD Zone.**

Monitoring Point	Peak DPM ( $\mu\text{g}/\text{m}^3$ )	Duration DPM $<160$ $\mu\text{g}/\text{m}^3$ (min)
Intake Airway Node	348	-
Return Airway Node	237	18
Exposure Face Node	87	62
LHD Zone Nodes	257	104
Mid-Point Junction Node	265	99

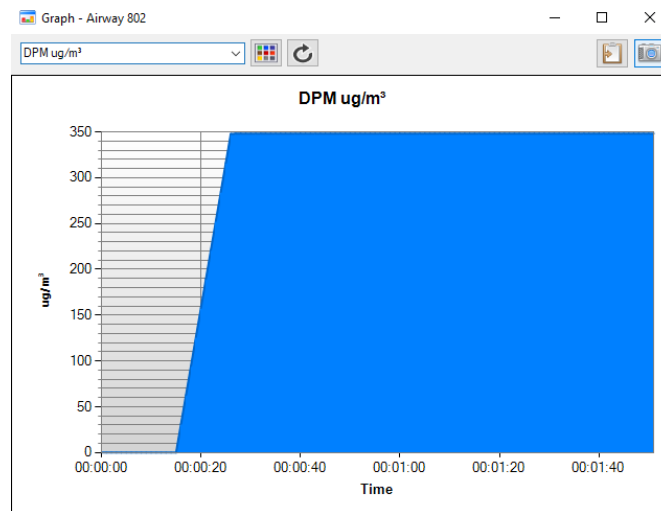


**Figure 27. Dynamic Simulation of DPM Dispersion at 2 Minutes of Diesel Operation at the 1<sup>st</sup> monitor.**

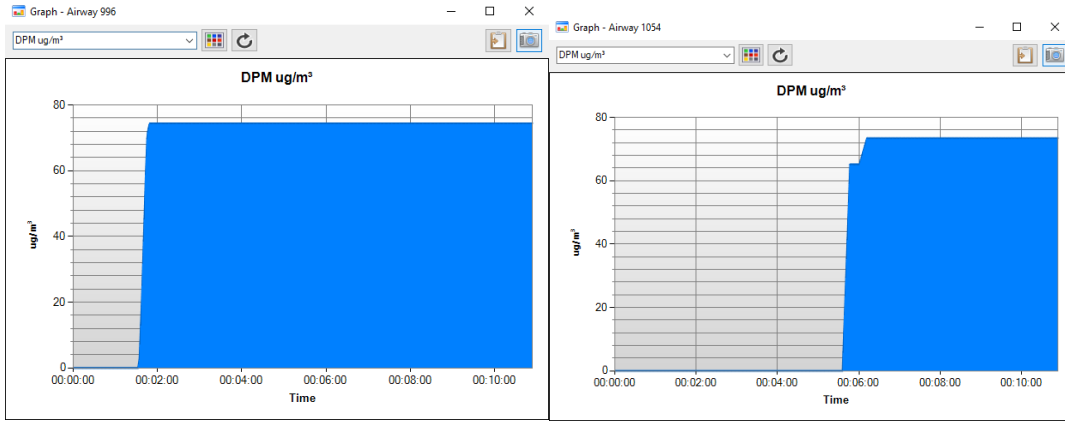


**Figure 28. Dynamic Simulation of DPM Dispersion at 15 Minutes of Diesel Operation at the 2<sup>nd</sup> and 3<sup>rd</sup> monitors.**

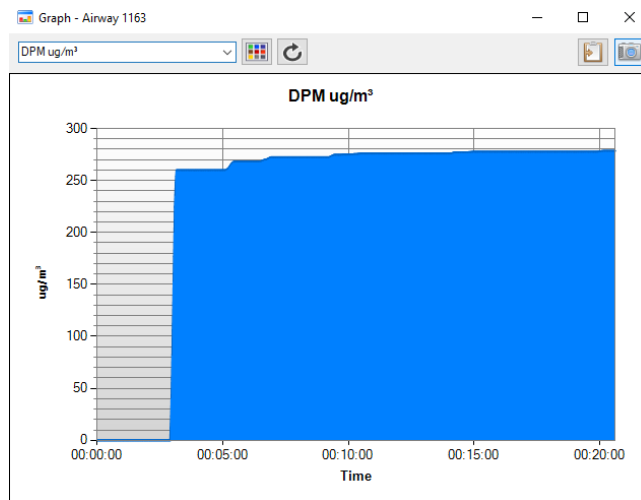


**Figure 29. Dynamic Simulation of DPM Dispersion at 20 Minutes of Diesel Operation at the 4<sup>th</sup> monitor.**

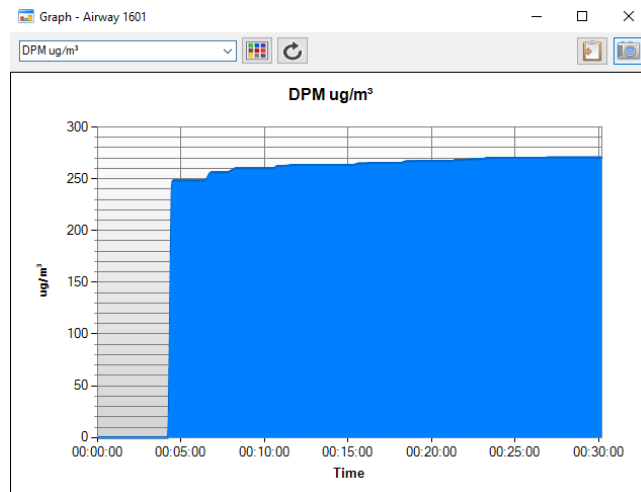


**Figure 30. Dynamic Simulation of DPM Dispersion at 30 Minutes of Diesel Operation at the 5<sup>th</sup> monitor.**

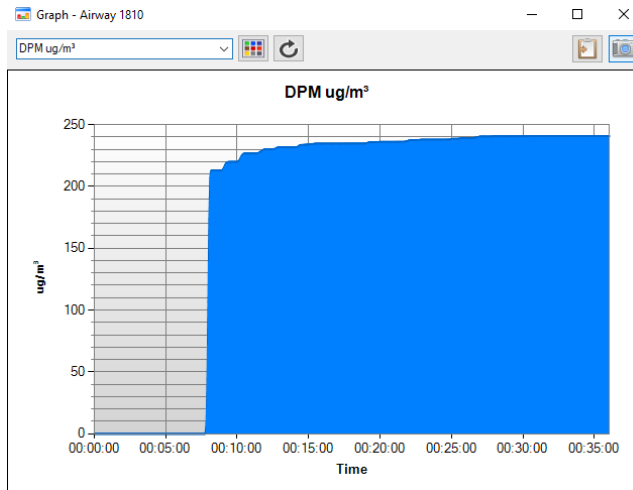


**Figure 31. Dynamic Simulation of DPM Dispersion at 35 Minutes of Diesel Operation at the 6<sup>th</sup> monitor.**

#### **4.4 Risk Analysis with Volumetric Methane Model**

The exposure methane was calculated using the Methane Model from @RISK, which aims to predict methane gas exposure from the coal bed. All 5 input data were sourced from credible references to replicate real-life scenarios. According to the Figure 33, using the inputs from the Figure 32, within the 90% confidence interval Methane Exposure is estimated to be between 267 m<sup>3</sup> to 1333 m<sup>3</sup>, however the most concentrated value is around 600 m<sup>3</sup>. The mean value is 700.23 m<sup>3</sup> and more values are concentrated around the mean, but the standard deviation is relatively large, 335.07 m<sup>3</sup>, there are significant deviations, especially toward the higher end of the exposure. The Figure 34 displays the comparison of actual to lognormal data (red line). The lognormal distribution is a good model for this exposure data since it closely fits the distribution of the output. As it is common, the lognormal distribution is skewed to the right, with a long tail extending toward the higher values and the majority of the values concentrated in the lower range.

The graph in the Figure 35 estimates how the factors affect the variance of exposure of methane gas. Gas content (m<sup>3</sup>/ton) plays a crucial role as more than a half of the variance depends on it. Although exposure factor and drainage area are far less important than gas content, they also play a big role. Meanwhile, density of coal and thickness of coal bed contribute relatively less, which means they have less impact on exposure volume.

The last graph in the Figure 36 is a tornado chart for the model. The x-axis shows the output mean, which is exposure ( $m^3$ ) and the y-axis demonstrates the input variables, which are affecting the output. It proves that density and thickness have hardly any effect on the output, whereas 3 other inputs affect the results mostly. Gas content's bar of low input reaching  $328.93 m^3$  and high input bar reaching  $1,142.37 m^3$  suggest that exposure is highly influenced by gas content, as there is a wide range of high and low readings. Another important factor influencing exposure is the exposure factor; a large input yields  $960.70$  while a low input yields  $448.30$ . Drainage Area has a modest effect on exposure, with a high input value of  $959.80$  and a low input value of  $490.99$ .

**Table 6. Values of given inputs to the Methane Model.**

Drainage Area ( $m^2$ )	166.7
Thickness (m)	3.9
Gas Content ( $m^3$ /tons)	3.7
Density ( $tons/m^3$ )	1.5
Exposure factor (fraction)	0.2

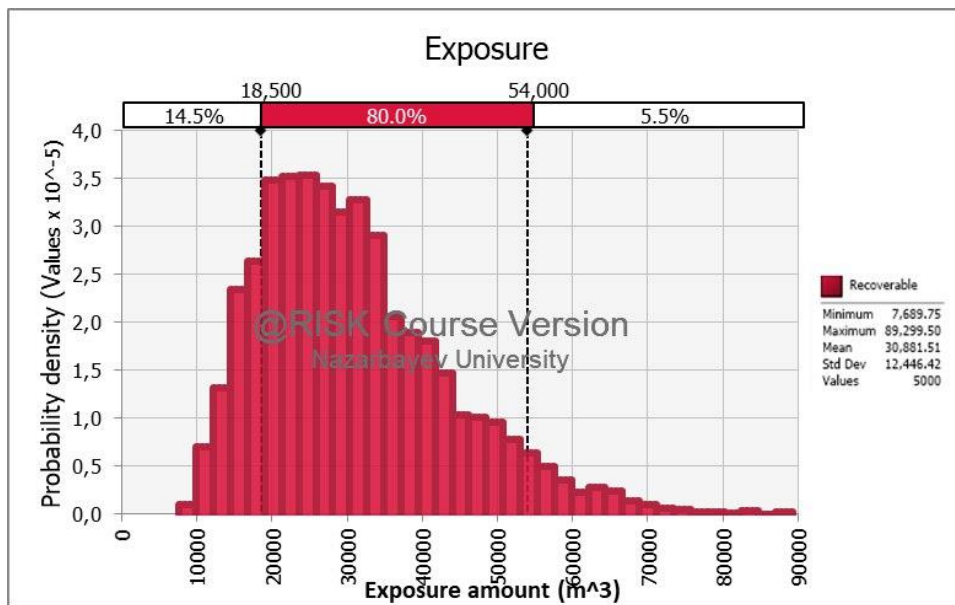


**Figure 32. Exposure of methane as predicted by the Methane Model.**

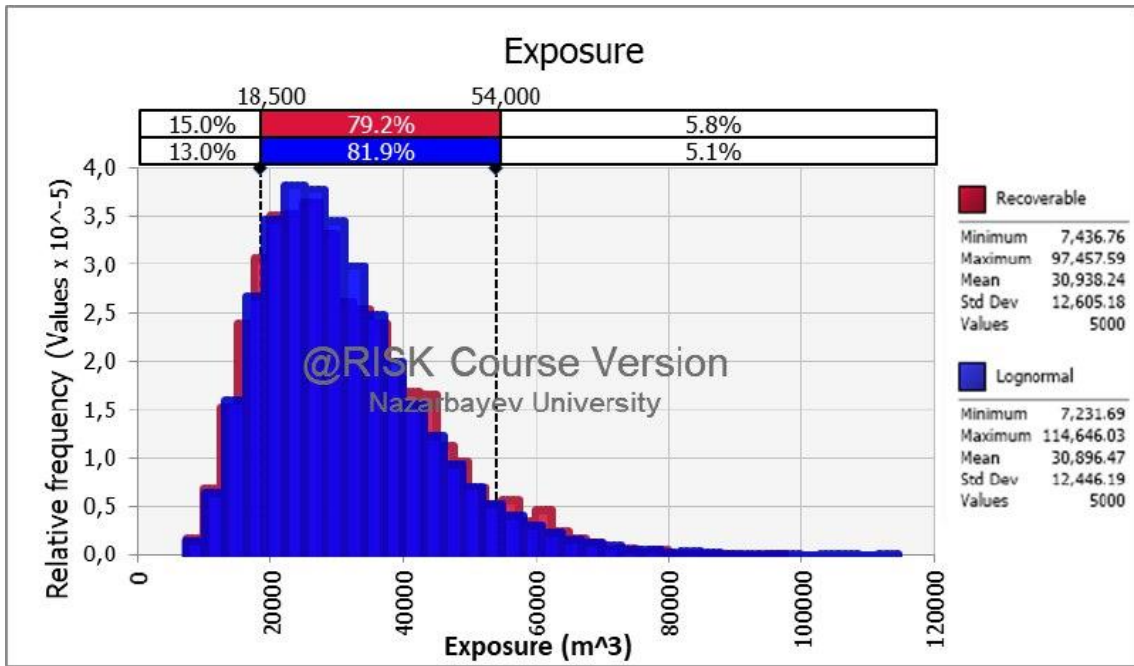


Figure 33. Fit comparison of methane exposure with Lognormal Distribution Model.

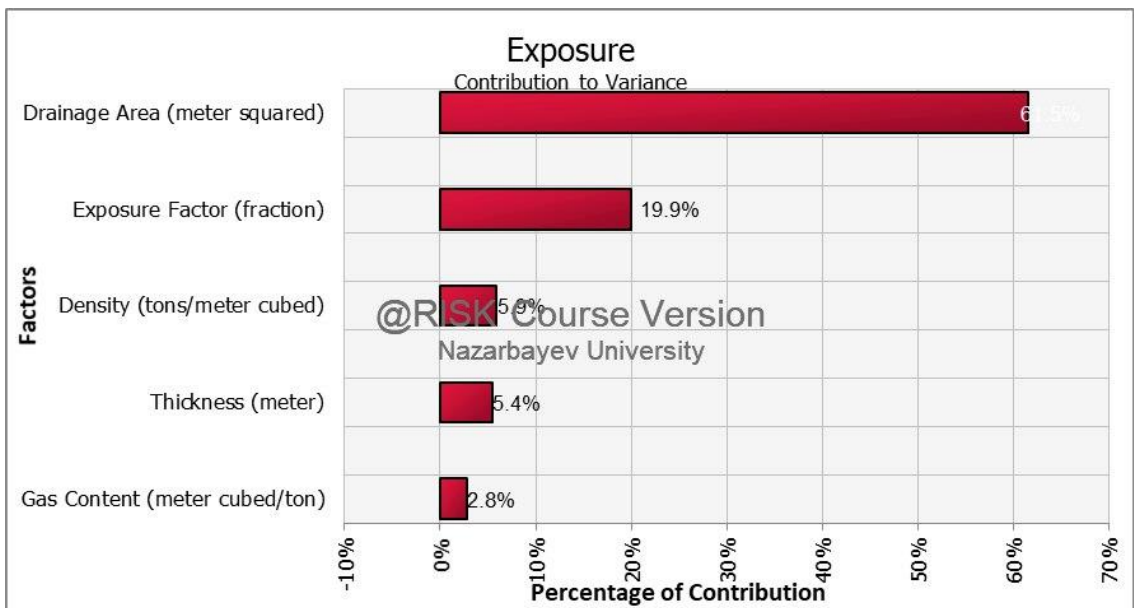


Figure 34. Contribution of factors to variance.

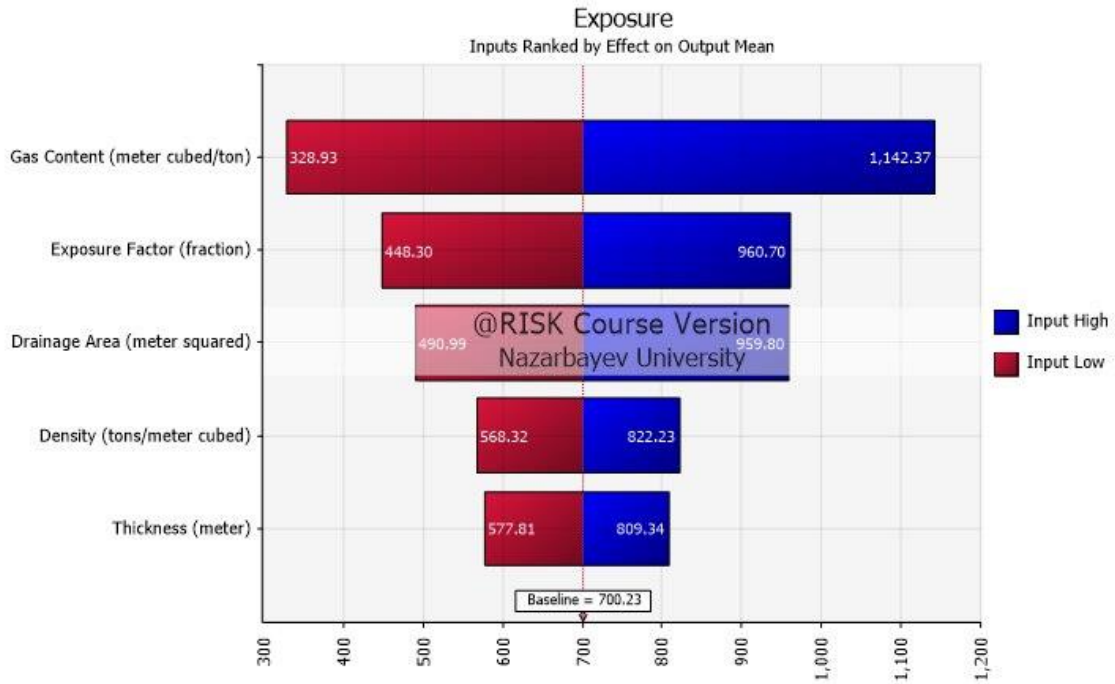


Figure 35. Tornado chart on the inputs.

Methane volume (in cubic meters) is calculated using the ventilation system's total air volume and the  $CH_4$  percentage by the following formula:

$$V_{CH_4} = \left( \frac{\%(CH_4)}{100\%} \right) * V_{air} \quad (1)$$

## 5. DISCUSSION

This study evaluated the performance of a dynamically simulated underground ventilation system under baseline, post-exposure, and diesel-intensive operational scenarios using VentSim DESIGN™. Each condition revealed distinct system behaviors, highlighting strengths and latent vulnerabilities within the room-and-pillar configuration.

Under baseline conditions, airflow velocities remained well-distributed, with primary headings averaging between 2.1 and 2.7 m/s. These values meet industry-accepted airflow targets for diesel-supported hard rock mining (Krause & Krzemień, 2014). The total modeled airway length of 110,479 meters and airflow delivery of 181.2 m<sup>3</sup>/s ensured a pressure-controlled flow regime, maintained by two fans with a combined power of 417.3 kW at 63.9% efficiency.

The post-exposure scenario focused on the simultaneous release of methane ( $CH_4$ ), nitrogen dioxide ( $NO_2$ ), and carbon monoxide ( $CO$ ) at the detonation site. Methane

reached a maximum of 0.8% at the Intake Node (Monitor #1). Figures 11–15 illustrate  $CH_4$ 's stratified rise and rapid dilution due to buoyancy-driven dispersion. These dynamics confirmed the expected vertical migration of  $CH_4$  under neutral thermal conditions and reinforced the utility of overhead airflows in mitigating flammable gas accumulation.

Nitrogen dioxide, by contrast, exhibited slower, ground-level migration, consistent with its greater density and lower diffusivity. At the Monitor #1,  $NO_2$  peaked at 3 ppm—well below the OSHA 5 ppm ceiling. These results underscore the need for booster ventilation or localized jet fans near methane exposure faces to prevent gas entrapment in low-mobility zones.

Carbon monoxide, which has intermediate dispersion behavior, showed faster lateral movement, reaching 30 ppm at the Intake Airway Node and 24 ppm at the Mid-Point Junction Node. Despite originating at the methane exposure face, peak values were higher downstream due to prevailing airflow direction and vortex formation. The CO concentration remained above the OSHA TWA of 25 ppm for up to 30 minutes in some regions with slow clearance attributed to recirculation patterns and junction-induced eddies.

These results collectively support Hypotheses 1 and 2: namely, that post-exposure events create zones of transient contaminant buildup that exceed safety thresholds even in the presence of baseline-compliant ventilation.

Dynamic snapshots (Figures 27–31) visualized the progressive spread of DPM from localized peaks at 20 minutes to broader contamination. This gradual saturation further supports the recommendation that mobile diesel equipment should be synchronized with dynamic ventilation adjustments, such as airflow rerouting or real-time sensor feedback systems.

Discussing the correlation between the Ventsim model and the Methane Model, developed using @Risk software, is crucial. In the future, if an engineer has precise information about the coal bed—such as its area and gas content—Ventsim could help estimate the volume of toxic gases circulating in that area. This would allow for more accurate predictions and effective management of gas exposure.

## 6. CONCLUSIONS

This research investigated the hazards associated with toxic gas accumulation in underground mining environments through the development and application of a dynamic, simulation-based assessment framework. Utilizing VentSim DESIGN™ and a realistically scaled, undisclosed room-and-pillar mine geometry, the study modeled three operationally distinct scenarios—baseline airflow, post-exposure gas release, and diesel equipment operation—to evaluate the ventilation network’s responsiveness to transient and sustained contaminant events.

The primary objective was to assess whether conventional steady-state ventilation designs provide sufficient protection against temporally and spatially variable gas emissions. This was accomplished by simulating the behavior of four high-risk airborne contaminants—methane ( $CH_4$ ), carbon monoxide (CO), nitrogen dioxide ( $NO_2$ ), and diesel particulate matter (DPM)—under different operational conditions, and evaluating concentration trends, clearance times, and airflow distribution patterns across the ventilation network.

Under baseline conditions, the simulation confirmed adequate ventilation performance in pollutant-free settings, with average airflow velocities exceeding 2.0 m/s in major drifts and pressure differentials supporting directional airflow toward the return airway. These outcomes aligned with industry standards and satisfied the first specific objective of evaluating system behavior in static conditions.

However, the dynamic simulation scenarios demonstrated significant deficiencies in system adaptability when exposed to time-sensitive gas surges and prolonged diesel emissions.  $CH_4$  concentrations approached the lower explosive limit (LEL), further affirming that standard ventilation alone may be insufficient in high-risk areas during short-term emission events.

The diesel operation scenario reinforced the second hypothesis, demonstrating how continuous emissions from LHD equipment generate sustained DPM and  $NO_2$  accumulation. At key locations—including the LHD Zone Node and Mid-Point Junction Node—exceedance durations surpassed 100 minutes, indicating persistent exposure hazards in geometrically disadvantaged ventilation zones. These findings

addressed the third specific objective, providing evidence of airflow stagnation and pollutant retention under chronic loading conditions.

The study also confirmed the third hypothesis: that dynamic simulation modeling using Ventsim™ effectively captures contaminant dispersion, identifies ventilation inefficiencies, and supports the development of targeted airflow improvements. The software's ability to simulate passive gas transport, thermal interactions, and scenario-specific emission profiles enabled spatially resolved analysis of pollutant behavior over time. This functionality was critical in evaluating gas migration trends, ventilation bottlenecks, and the delayed clearance patterns observed across scenarios.

Taken together, the results emphasize the limitations of threshold-based, fixed ventilation designs and advocate for adaptive, feedback-driven ventilation control strategies. Specifically, the delayed clearance of toxic gases in key nodes suggests the need for real-time monitoring integration, supplemental booster ventilation in high-emission zones, and dynamic zoning aligned with equipment location and operational cycles. These measures would enhance the system's ability to respond to transient emission risks, reduce worker exposure, and ensure more consistent compliance with occupational health standards.

Although the research utilized a modeled mine configuration and literature-informed emission values, the conclusions are directly applicable to mid-scale mechanized mining operations employing room-and-pillar extraction methods. The methodology provides a transferable blueprint for assessing ventilation effectiveness under various emission conditions, enabling mining engineers to test ventilation responses without the safety risks or logistical constraints of field experimentation.

## **7. RECOMMENDATIONS**

Several limitations must be acknowledged. These include the absence of empirical calibration data, the use of passive scalar transport rather than full turbulence modeling, and the exclusion of gas reactivity or sorption effects. As such, while absolute concentration values should be interpreted with caution, the relative behavioral patterns and clearance trends offer meaningful insight into system performance under stress conditions.

Future research should focus on integrating real-time sensor data with simulation platforms to support predictive ventilation management. Empirical validation studies across active underground sites are essential for refining model accuracy. Furthermore, hybrid modeling approaches combining VentSim with CFD tools or machine learning algorithms may offer improved resolution in capturing transient gas behavior and flow field complexity. Interdisciplinary collaboration across mining engineering, occupational hygiene, and data science domains will be key to advancing the next generation of intelligent mine ventilation systems.

In conclusion, this thesis achieved all stated objectives and validated its core hypotheses through rigorous scenario-based modeling. It establishes that conventional ventilation systems, while compliant under nominal conditions, exhibit vulnerabilities when exposed to realistic operational variability. The research contributes substantively to the evolving discourse on adaptive mine ventilation, offering both theoretical advancements and practical guidance for enhancing underground air quality management and toxic gas hazard mitigation.

## 8. REFERENCES

- Anas, M., Haider, S. M., & Sharma, P. (2017). Gas monitoring and testing in underground mines using wireless technology. *Int. J. Eng. Tech. Res*, 6, 412–416.
- Asfaw, A., Mark, C., & Pana-Cryan, R. (2013). Profitability and occupational injuries in US underground coal mines. *Accident Analysis & Prevention*, 50, 778–786.
- Chang, H., Meng, X., Wang, X., & Hu, Z. (2024). Research on coal mine longwall face gas state analysis and safety warning strategy based on multi-sensor forecasting models. *Scientific Reports*, 14(1), 13795.
- Chen, Y., Silvestri, L., Lei, X., & Ladouceur, F. (2022). Optically powered gas monitoring system using single-mode fibre for underground coal mines. *International Journal of Coal Science & Technology*, 9(1), 26.
- Chećko, J., Howaniec, N., Paradowski, K., & Smolinski, A. (2021). Gas migration in the aspect of safety in the areas of mines selected for closure. *Resources*, 10(7), 73.
- Fan, Z., & Xu, F. (2021). Health risks of occupational exposure to toxic chemicals in coal mine workplaces based on risk assessment mathematical model based on deep learning. *Environmental Technology & Innovation*, 22, 101500.
- Ge, L., Zhang, Z., Wang, Y., Zhang, S., & Chen, Y. (2024). Investigation on a mobile fire extinguishing approach using liquid carbon dioxide as inert medium for underground mine. *PLOS ONE*, 19(4), e0299940.
- Gong, W., Hu, J., Wang, Z., Wei, Y., Li, Y., Zhang, T., ... & Grattan, K. T. (2022). Recent advances in laser gas sensors for applications to safety monitoring in intelligent coal mines. *Frontiers in Physics*, 10, 1058475.
- Huang, S., Li, Z., Li, L., & Wu, J. (2025). Characteristics of Harmful Hot Gas Group Migration and Ventilation Control after Mine Explosion. *ACS Omega*.
- Jia, R., & Nie, H. (2017). Decentralization, collusion, and coal mine deaths. *The Review of Economics and Statistics*, 99(1), 105–118. [https://doi.org/10.1162/REST\\_a\\_00563](https://doi.org/10.1162/REST_a_00563)
- Jo, B. W., Khan, R. M. A., Lee, Y. S., Jo, J. H., & Saleem, N. (2018). A Fiber Bragg Grating-Based Condition Monitoring and Early Damage Detection System for the

Structural Safety of Underground Coal Mines Using the Internet of Things. *Journal of Sensors*, 2018(1), 9301873.

Karacan, C. Ö., Ruiz, F. A., Cotè, M., & Phipps, S. (2011). Coal mine methane: A review of capture and utilization practices with benefits to mining safety and to greenhouse gas reduction. *International Journal of Coal Geology*, 86(2–3), 121–156.

Keshamoni, K., Rao, G. K., Satheesh, B., & Priyanka, P. (2024, February). Revolutionizing Gas Safety: The IoT Gas Detector with Automatic Regulator Control. In *2024 4th International Conference on Innovative Practices in Technology and Management (ICIPTM)* (pp. 1–6). IEEE.

Krause, E., & Krzemień, K. (2014). Methane risk assessment in underground mines by means of a survey by the panel of experts (SOPE). *Journal of Sustainable Mining*, 13(2), 6–13.

Kumar, A., Kingson, T. M. G., Verma, R. P., Kumar, A., Mandal, R., Dutta, S., ... & Prasad, G. M. (2013). Application of gas monitoring sensors in underground coal mines and hazardous areas. *International Journal of Computer Technology and Electronics Engineering*, 3(3), 9–23.

Li, H., Zhang, Y., & Yang, W. (2023). Gas explosion early warning method in coal mines by intelligent mining system and multivariate data analysis. *PLOS ONE*, 18(11), e0293814.

Liang, R., Zhang, C., Huang, C., Li, B., Saydam, S., Canbulat, I., & Munsamy, L. (2024). Multimodal data fusion for geo-hazard prediction in underground mining operation. *Computers & Industrial Engineering*, 193, 110268. <https://doi.org/10.1016/j.cie.2024.110268>

Lin, B., Huang, Y., Yang, W., & Zhang, Y. (2020). Real-time methane prediction in underground longwall coal mines using artificial intelligence. *Energies*, 15(17), 6486. <https://doi.org/10.3390/en15176486>

Menéndez, J., Merlé, N., Fernández-Oro, J. M., Galdo, M., Álvarez de Prado, L., Loredó, J., & Bernardo-Sánchez, A. (2022). Concentration, propagation and dilution of toxic gases in underground excavations under different ventilation modes. *International Journal of Environmental Research and Public Health*, 19(12), 7092. <https://doi.org/10.3390/ijerph19127092>

Narkhede, P., Walambe, R., Mandaokar, S., Chandel, P., Kotecha, K., & Ghinea, G. (2021). Gas detection and identification using multimodal artificial intelligence based sensor fusion. *Applied System Innovation*, 4(1), 3.

Olczak, M., Piebalgs, A., & Balcombe, P. (2023). A global review of methane policies reveals that only 13% of emissions are covered with unclear effectiveness. *One Earth*, 6(5), 519–535.

Osunmakinde, I. O. (2013). Towards safety from toxic gases in underground mines using wireless sensor networks and ambient intelligence. *International Journal of Distributed Sensor Networks*, 9(2), 159273.

Rahimi, S., Atae-Pour, M., & Madani, H. (2022). CFD modeling of impact of gas content uncertainty on methane distribution in underground coal mine roadways. *Journal of Mining & Environment*, 13(2), 493–502. <https://doi.org/10.22044/jme.2022.11696.2158>

Raheem, S. R. (2011). Remote monitoring of safe and risky regions of toxic gases in underground mines: A preventive safety measures. *Postgraduate Diploma Thesis Report*, African Institute for Mathematical Sciences (AIMS), South Africa.

Sadeghi, S., Soltanmohammadlou, N., & Nasirzadeh, F. (2022). Applications of wireless sensor networks to improve occupational safety and health in underground mines. *Journal of Safety Research*, 83, 8–25.

Semin, M., & Kormshchikov, D. (2024). Application of artificial intelligence in mine ventilation: A brief review. *Frontiers in Artificial Intelligence*, 7, 1402555.

Tutak, M., Krenický, T., Pirník, R., Brodny, J., & Grebski, W. W. (2024). Predicting methane concentrations in underground coal mining using a multi-layer perceptron neural network based on mine gas monitoring data. *Sustainability*, 16(19), 8388.

Vallejo-Molina, L., Blandon-Montes, A., Lopez, S., Molina-Escobar, J., Ortiz, A., Soto, D., ... & Molina, A. (2024). Application of artificial intelligence to the alert of explosions in Colombian underground mines. *Mining, Metallurgy & Exploration*, 41(4), 2129–2142.

Wang, D., Zhang, P., Zhang, Y., Tu, S., Wang, J., & Hao, Z. (2022). Distribution characteristic and migration mechanism of toxic gases in goafs during close-distance coal seam mining: A case study of shaping coal mine. *ACS Omega*, 7(8), 7403–7413.

Wu, B., Meng, Y., He, B., Zhao, C., & Lei, B. (2022). Study on the migration law of gas explosion disaster products in complex air network of mine. *Energy Sources, Part A: Recovery, Utilization, and Environmental Effects*, 44(3), 6378–6391.

Wu, R. M., Shafiabady, N., Zhang, H., Lu, H., Gide, E., Liu, J., & Charbonnier, C. F. B. (2024). Comparative study of ten machine learning algorithms for short-term forecasting in gas warning systems. *Scientific Reports*, 14(1), 21969.

Yang, Y., Yang, S., Li, Z., Fang, Q., Wu, J., Cai, J., & Sun, W. (2020). Analysis of Hazard Area of Dispersion Caused by Leakage from Underground Gas-Storage Caverns in Salt Rock. *Advances in Civil Engineering*, 2020(1), 8876646.

Zhang, Y., Guo, H., Lu, Z., Zhan, L., & Hung, P. C. (2020). Distributed gas concentration prediction with intelligent edge devices in coal mine. *Engineering Applications of Artificial Intelligence*, 92, 103643.

Zheng, C., Jiang, B., Xue, S., Chen, Z., & Li, H. (2019). Coalbed methane emissions and drainage methods in underground mining for mining safety and environmental benefits: A review. *Process Safety and Environmental Protection*, 127, 103–124.

Ziętek, B., Banasiewicz, A., Zimroz, R., Szrek, J., & Gola, S. (2020). A portable environmental data-monitoring system for air hazard evaluation in deep underground mines. *Energies*, 13(23), 6331.